Random Walk of pVIc Peptide on Confined, Two-Dimensional DNA-Origami Carpets

Pascal Freyer

18 July 2013

Bachelor thesis, submitted to the faculty of

Mathematics and Natural Sciences
Rijksuniversiteit Groningen

as requirement to fulfilling the degree of Bachelor of Science in Physics.

Prof. Dr. Antoine M. Van Oijen, first advisor
Dr. Torben Cordes, second advisor

Single-Molecule Biophysics
Zernike Institute for Advanced Materials
Rijksuniversiteit Groningen
The Netherlands

Abstract

This thesis is a follow-up of single-molecule studies that have characterized one dimensional random walk of the 11 amino-acid peptide pVIc along DNA. It was originally aimed at obtaining further insight to pVIc sliding on two dimensional DNA-origami sheets with characteristic size of 50nm x 150nm. Making use of TIRF microscopy and custom analysis software, particle trajectories could theoretically be obtained at accuracies around 20 nm. This accuracy could however not be utilized due to large (80nm) spatial oscillations of the field of view (FOV), that remain unexplained. In addition, from the one-dimensional diffusion constant of pVIc a predicted camera exposure times of maximum 20us would be necessary to make appropriate MSD graphs and determine the two-dimensional diffusion coefficient. As this was not possible (camera exposure time minimum of 2,4ms for stream acquisition (movies)), we tried to extract quantitative information from the Gaussian fits of the fluorescent spots. I will present these results including the typical trajectories that pVIc shows at 16ms exposure time, with the mentioned FOV oscillations. I hope to give a good picture of the ups and downs of analysing a large number of molecules simultaneously and the obstacles that need to be overcome in order to obtain more meaningful results.

Acknowledgements

I thank Prof. Dr. Antoine M. van Oijen, Dr. Torben Cordes and Alex Turkin for continuous input throughout the course of my experiments and reviewing my thesis report. Especially Alex Turkin for teaching me everything that I needed to know in the lab, microscope basics, and guiding me where necessary. Lei Zhang for Biotinylated DNA-origami sheets and AFM images. Sarah Stratmann for PDMS and materials. Michiel Punter for software support and Dr. Victor Krasnikov for hardware support concerning microscope and camera. Last but not least, thank you to the whole SMB group for helping me out here and there and improving my presentation, but most importantly for giving me a valuable insight into the act of 'doing research'.

Contents

Table of contents:

List of figures/ tables:

Introduction

Life can only function due to very specific molecular interactions taking place: very specific chemical reactions that are catalysed by proteins that need to find their target sites within a chaotic micro-molecular world. This is also true for processes involving DNA, such as gene transcription, and DNA repair processes within a cell.

Already in 1970 scientists discovered that some proteins would find their target on DNA much faster than three dimensional diffusion theory would allow. It was predicted that sliding along DNA would reduce the dimensionality of the search process, thereby speeding it up [1]. Today we know this is actually true for several proteins of various type [2, 3, 4] and the question has progressed to: how exactly do they do this? Several possible processes were summarised by Van Oijen et al. in 2011 [1].

The group I have done this project in is currently busy unravelling the precise mechanism that lies behind the activation process of adenovirus proteinase (AVP) which takes place in the late infection cycle of the human Adenovirus. AVP is essential for processing viral precursor proteins used in virus assembly [4]. But to do so it has to find these precursors inside an environment of extreme density of DNA (>500 g/litre) that exists inside the virus, and what could now be a better method than sliding along this DNA?! In fact it has not developed the ability to slide along DNA itself, but it *acquires* this novel ability from another protein called protein VI (pVI). pVI is a multifunctional protein, but here we focus on its role of activating AVP, as well as giving off its ability to slide along DNA to AVP. This process is described by Mangel et al. [5] who found out that this can happen through peptide pVIc, the last eleven C-terminal amino acids of pVI, being cleaved off pVI and then bound to AVP. In other words, pVIc gives the ability to slide along DNA from pVI to AVP. It does not only give this ability, it can also slide along DNA by itself.

Understanding the sliding mechanism of this, mere eleven amino-acid long, pVIc peptide would of course be a great thing and reproducing such a trait would certainly have a good chance of finding a number of applications in the bio-engineering world. Certainly if you see DNA, the “rail road” of pVIc, as an extremely versatile and promising material for nano-scale bio-engineering. Well, how is it possible to answer this question that does not only apply to pVIc but many other proteins as well? Questions like: What is the mechanism that allows proteins to slide along DNA? Do they slide at all, or do they move forward by hopping along DNA? Do they travel along the helix backbone or not? The latter questions are difficult to find an answer to if we cannot visualize the molecule itself, and that is how we inevitably come to the field of single-molecule imaging.

A common principle that all single-molecule techniques have, is the use of fluorophores, that act as a light emitting signalling or tracking tool and are attached to or interact with the molecule of interest. Like this we can track single molecules and/or their behaviour and thus learn about their mechanisms in a more specific detail than bulk experiments. Recent single-molecule experiments of proteins sliding along DNA were able to answer some of these questions [2, 3, 4]. For example tumour suppressor protein p53 is found to slide along DNA and not hop. Furthermore, the use of experimental finding and theoretical upper limit of the diffusion coefficient, allowed quantitative assessment of the free energy landscape of p53 sliding [3].

Now, to come back to my project, we would like to study this adenovirus chain of reactions involving the pVIc “molecular sled”. How would we do this? Look at the entire Adenovirus? That is an approach that we could classify as “top-down” in this context, which would certainly be interesting. However the “bottom-up” approach is what we chose for simplicities sake. Even a very simple biological system like a virus already has a great deal of complexity which we are not interested in quite yet. Looking at pVIc sliding along DNA “one dimensionally” was already done in my research group, so the next step would be to look at a more realistic compact-DNA environment in three dimensions. Everyone working in this field knows that this is already a big step, but what lay at hand was to use the same setup, used already for one dimensional sliding, and combine it with the

use of DNA-origami sheets, which would provide us with a “two dimensional” sliding platform for pVIc.

This is exactly what we did here. Using total internal reflection (TIRF) microscopy, we visualised fluorescently labelled pVIc binding to two dimensional DNA-origami sheets. These origami sheets were 150nm x 50nm in size and attached to the glass coverslip surface by biotin-streptavidin-biotin linkers.

Methods and Materials

Theory and what I expect to find

-Centroid determination

For determining the position of the fluorescent spot in two dimensions, the fluorescent spot intensity profile is fitted with a two dimensional Gaussian distribution. Further parameters used in the following data analyses are derived from this Gaussian fit. The centre of the Gaussian fit depends on the photon count and background intensity. Position accuracy can be as low as 10 – 20 nm [3] but for our experiments this could lie well around 20 – 50 nm [6].

-Mean square displacement (MSD)

Isotropic diffusion, also called *un-biased random walk*, can be expressed in terms of the mean square displacement (MSD) of the particle and the time it takes to make this displacement:

$$MSD_{2D} =< r^2 >= 4Dt \qquad \textbf{(1)}$$

From the two dimensional position coordinates of a particle over time we can determine the MSD. This is well described by Schweizer [7] and can be expressed in terms of discrete time steps as equation 2:

$$MSD_{2D} = \frac{\sum_{i=1}^{N-n} (r_{i+n} - r_i)^2}{N-n} = 4Dn\,(\triangle t) \qquad \textbf{(2)}$$

Where r_i is the position coordinate in two dimensions for i^{th} time frame, n is the time frame number that we are analysing, n=1 being the first frame of the trajectory and N the total number of frames in the trajectory. The two-dimensional diffusion coefficient (D) can then be determined from the graph of MSD as a function of time n(Δt), whose slope is equal to 4D. As a note of good practise: The latter half of the MSD points are usually neglected in analysis because they are statistically not well enough supported.

As we are working with a confined area of diffusion (of pVIc on a DNA-origami sheet) we expect to get a line that flattens towards a horizontal as n becomes larger. This is due to pVIc having reached the maximal displacement it can make within the origami confinement. The slope of the first linear part of the MSD curve is used for determining D in this case because it still corresponds to the unaffected, free diffusion of pVIc within its two-dimensional space.

Not being able to obtain the wanted MSD curve, we employed different methods to extract quantitative conclusions from the data. The following analyses were used.

-Full-width-at-half-maximum (FWHM) analysis.

The fluorescent spot that is acquired in one time frame is the sum of all the photons that one single fluorophore emits into the direction of the camera within 16,01ms (camera exposure time). The *intensity distribution* of this spot can be mathematically expressed as the convolution of the *fluorophore intensity distribution* and the *spatial distribution* of this fluorophore. The fluorophore intensity distribution is given by the intensity profile of a perfectly still fluorophore, the spatial distribution is given by the spatial distribution of the fluorophore position (which fluctuates) over time. When written in terms of the FWHM this can be expressed in the form of equation 3.

$$(FWHM_{spot}) = \sqrt{(FWHM_{fluoroph.int.})^2 + (FWHM_{spatial})^2} \quad \textbf{(3)}$$

In our analysis the background signal and camera electronic noise contribution are neglected, as well as the consideration that two or more particles can look like one single particle.

We expect to see two peaks in a histogram of all the detected spots' FWHM values. One peak due to the population of stuck, spatially more confined population of pVIc molecules, and the other peak from the pVIc molecules sliding on the DNA-origami.

-Trajectory lifetime analysis.

Similar to the FWHM histograms, we also made histograms of the trajectory lifetimes in order to see whether there would be distinct behaviours of sliding lifetimes, especially when comparing an experiment with origami sheets and a negative control (without origami sheets). If there is another population with a differing lifetime in the presence of DNA-origami, we should be able to see this by looking at these distributions. A double-exponential fit of the distributions would give us quantitative evidence. If these fits give us differing lifetime constants between the different experiments, then this suggests differing lifetime populations. When the two lifetime constants for a double exponential fit are equal, they represent the same lifetime population and should both be equal to the lifetime constant of a single-exponential fit. This suggests the presence of only one lifetime population.

The characteristic lifetime constants can also be determined from fitting a single logarithmic scale graph of the lifetime distribution with one straight line or two straight lines. In the case of two inclines, this would give two characteristic lifetime constants for the two different particle populations: the sliding pVIc population and the stuck pVIc population.

Software

-ImageJ and the *Single Molecule Biophysics* plugin. More specifically:
Peak Fitter: to fit all intensity peaks with a two dimensional Gaussian and recording the centre position and other parameters such as the FWHM value.
Particle Tracker: links the peaks, located in Peak Fitter, together into a trajectory. The way that a set of peaks is combined to one trajectory can be adjusted by adjusting a number of selection parameters.

-*MATLAB*, *Microsoft EXCEL* and *OriginPro* for data analysis and graphing.

Sliding assay preparation and procedure

-PDMS flow cell description.

Polydimethylsiloxane (PDMS) is a soft polymer that can be moulded into forms of various kind. Very accurate forms can be made in this way by using accurate moulds that are created with photolithographic methods. I have used a rectangular PDMS block with a single microfluidic channel moulded into one of its sides (figure 1a). The PDMS block is of such a form, that it fits perfectly onto a 24mm x 24mm glass coverslip and into a holding clamp (figure 1b) that is placed into the microscope-mounted stage. (Also see the description in the students' lab journal on 23.04.2013, page 4.)

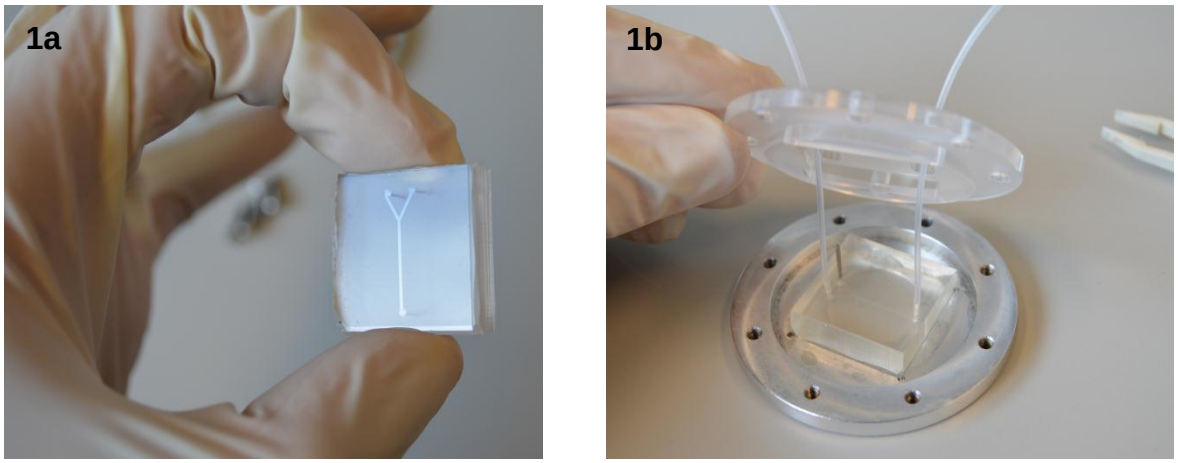

Figure 1. **The flow cell made of PDMS and a holding clamp for the microscope.** **1a** shows the flow channel becoming well visible against the reflection of light from the coverslip. The coverslip is already incubated with Streptavidin blocking buffer solution and attached to PDMS at this stage. **1b** shows the PDMS-coverslip unit placed inside the microscope holding clamp. Tubing is connected to opposite sides of the channel and one of the Y-junctions on the inlet side is blocked with a metal pin.

-References to the procedure of functionalizing glass coverslips.

We have used a similar silanisation protocol as described in *Methods in Enzymology* [8] with some variations in PEGylation solution (step number 5), that have been applied by Paul Blainey (see detailed description in the students' lab journal on 01.05.2013, page 8). Biotin-PEG-NHS 1mg/mL, NHS-PEG-NHS 10mg/mL, m-PEG-NHS 100mg/mL in sodium bicarbonate ($NaHCO_3$) 0,1M pH 8,3. Where 50µL was used per glass coverslip (24mm x 24mm).

-Procedure of preparing the flow cell for imaging.

To assemble the flow cell and attach DNA-origami to the – already functionalised – coverslip surface I used the procedure described by Van Oijen et al. [3, supplementary]. This involves the following steps in chronological order (see students lab journal for details of specific experiments):

-Blocking buffer (BB): Tris 20mM, EDTA 2mM, NaCl 50mM, BSA 0,2mg/ml, Tween-20 0,005%; pH 7,5 (where Tween-20 and BSA are stored as cooled stock solution in 5 times higher concentration and diluted with the right working buffer for every experiment).

-Degassing BB, incubating Streptavidin for 30min, washing PDMS and assembling flow cell.
-Incubating coverslip with 50µL of DNA-origami 18pM in BB for 3 x 15min. Washing with BB before and after and making sure that air bubbles are flushed out and do not enter the flow channel.

-Sliding buffer (SB): EDTA 0,05mM, NaCl 2mM, Glycerol 0,05%, Ethanol 20mM, HEPES 10mM; pH 7,0.

-pVIc-Cy3b 0,5nM in SB, degassed.
-YOYO 30nM in SB, degassed.

-The imaging procedure.

The syringe pump at the microscope (*New Era Pump Systems, Inc*.) is used to pump (pull) the prepared solutions out of the test tube and through the flow channel via an air spring, which evens out any sudden pressure changes and pressure fluctuations (figure 2).

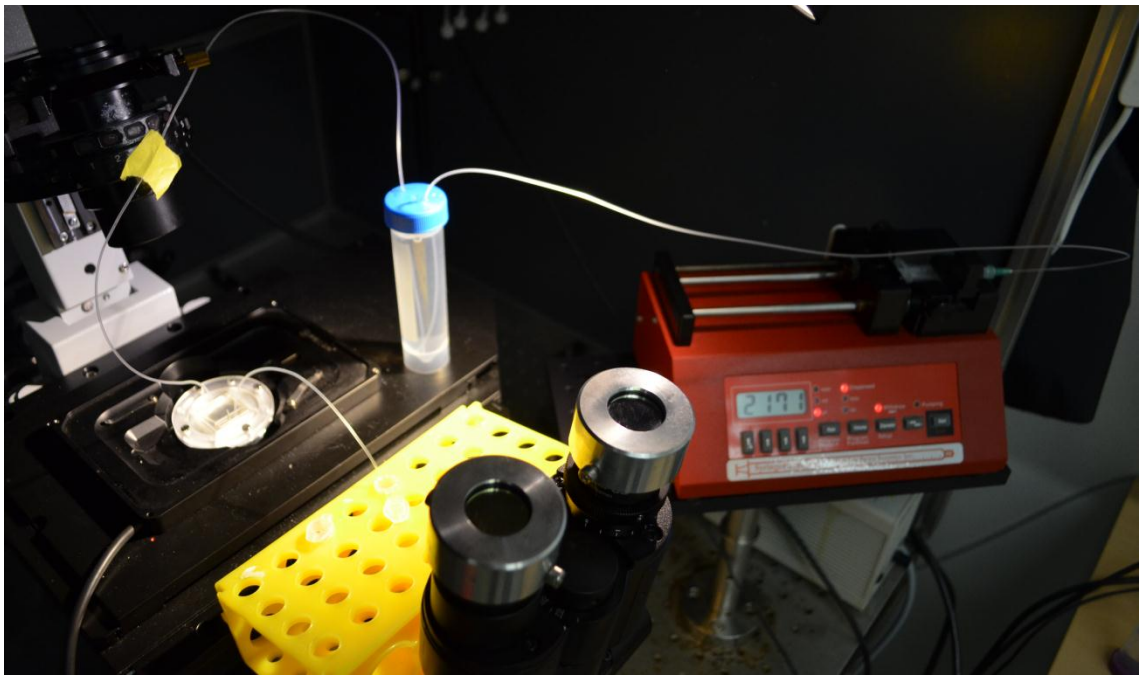

Figure 2. **Microscope setup**. From left to right along the 0,7mm diameter tubing (transparent-white) we can see: first the test tubes (in the yellow test tube rack), then the flow cell (round object), the air spring (large test tube with blue lid) and finally the syringe that is mounted on the syringe pump (red).

Protein labels, fluorescent dyes

The pVIc peptide is labelled with Cy3b organic fluorophore. In the Streptavidin-Cy5 control experiment we have used streptavidin labelled with Cy5 organic fluorophore. YOYO DNA-intercalating dye is an organic fluorophore that binds covalently to DNA, thereby altering the DNA's structure.

DNA-origami sheets

The DNA that is attached to the coverslip surface is a 50nm x 150nm DNA-origami sheet, like a carpet. An AFM picture of the origami sheet that I used is shown in figure 3a.

The structure of this origami sheet is effectively a number of side by side, stacked double helixes that are parallel to each other. Similar to the way described by Rothemund [9]. The origami sheets contain six biotin "anchors" (figure 3b) which will bind to the coverslip-bound streptavidin, thereby fixing the origami sheet to the coverslip surface.

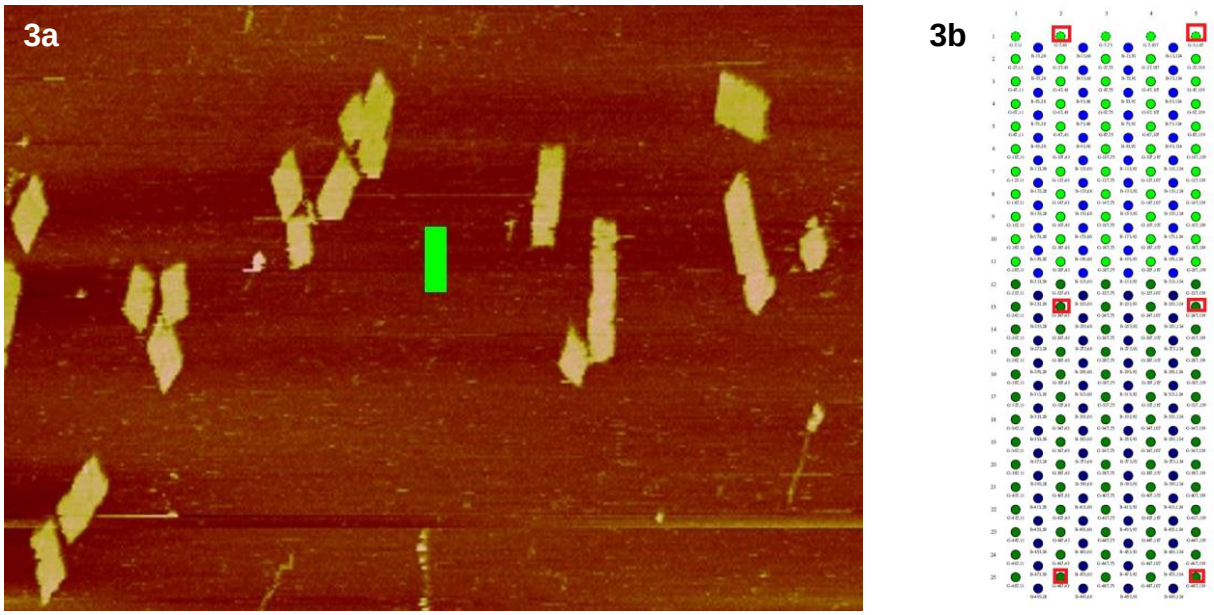

Figure 3. **Rectangular DNA-origami sheets. 3a** shows an AFM picture of the same origami sheets that we have been using in the experiments. The scale bar in green is 50nm x 150nm in size. **3b** indicates the position (in red) of the six biotin molecules bound to the rectangular origami sheet (green and blue dots).

Total internal reflection fluorescence (TIRF) microscope setup

- *Olympus* inverted optical microscope, model *IX71*, with a 100X oil immersion objective.

- *Hamamatsu* Digital EM-CCD (electron multiplier - charge coupled device) camera, model *C9100-13*, which has a 512pixels x 512pixels (16µm x 16µm per pixel) chip. We used a field of view (FOV) of 256pixels x 256pixels for acquiring all the data that was analysed in this thesis. This choice of FOV allowed a stream (continuous) acquisition with 16,01ms exposure time. A lower exposure time would require a FOV with less pixels, for example 4,21ms can be reached by using a FOV with 32 rows of pixels. Movie pixel size lies at:

Chip pixel size/ objective magnification = 16µm/100 = 160nm = $1{,}6*10^{-7}$m

- *Coherent* lasers, model *Sapphire* (OPSL-type laser), have been used for excitation of fluorophores. YOYO, Cy3b and Cy5 were excited with lasers of 488nm (blue light), 532nm (green light) and 643nm (red light) wavelength respectively.

- Optical density (OD) filters (also known as neutral density filters) for the adjustment of the laser power/ intensity, together with a set of mirrors and lenses for guiding the laser beam into the microscope and finally into its objective.

- A separate *filter set* is used for each laser wavelength. The aim of the filter set is to guide and filter the light, so that only excitation light can enter the objective and only emitted light (from the fluorophore) can leave the objective and enter the camera. For 643nm we are using a complete set: exciter filter, dichroic mirror and emission filter. For 532nm and 488nm only the dichroic mirror and emission-filter are used.

Results and Discussion

With the TIRF microscopy setup described, we acquired movies at 16,01ms exposure times per movie frame. The data analysis is done with tree different types of experiments: the *origami experiment* that contained DNA-origami sheets and pVIc-Cy3b sliding buffer, the *negative control experiment* that was identical to the origami experiment but did not include any origami sheets, and the *streptavidin-Cy5 control experiment* that used no origami sheets but streptavidin-Cy5 (see students' lab journal for details). The streptavidin-Cy5 control is an attempt to characterise molecules of which we know that they are stuck to the coverslip and do not slide.

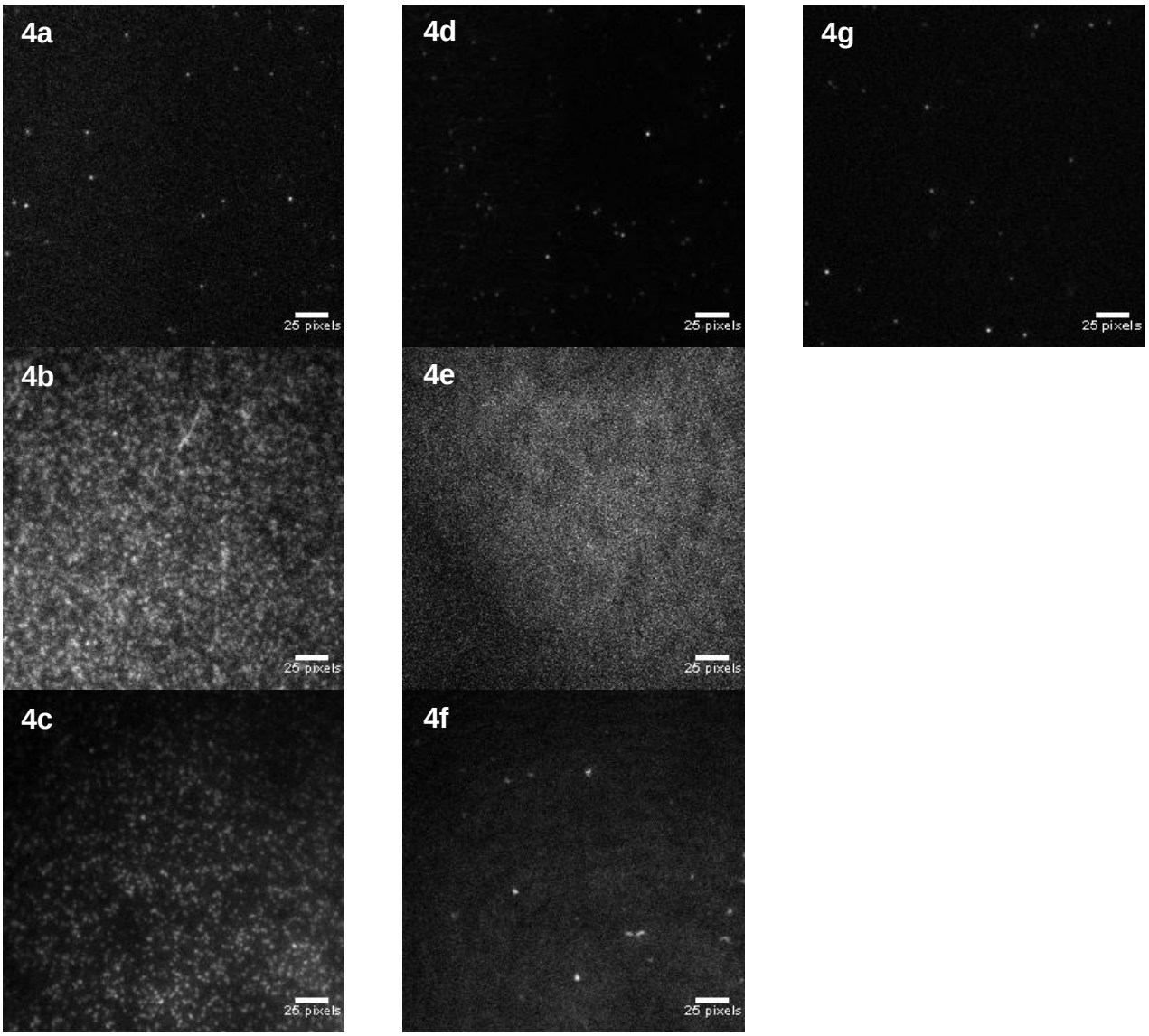

Figure 4. **One-frame selections out of the recorded particle movies.** The scale bars are 25pixels = 4µm long. **4a** is from an experiment with origami showing pVIc-Cy3b as white fluorescent spots. **4b** is the YOYO-control of the same experiment showing a very high coverage of origami sheets (clustering of white). **4d** is from a negative control experiment with pVIc-Cy3b and **4e** its respective YOYO-control showing no clustering but uniform background as expected (the grey-value variation is due to misaligned optics and background noise). **4c and 4f** are from a DNA control experiment in which we confirmed the DNA coverage findings in 4b and 4e respectively. The white spots in 4f are not supposed to be DNA because this was only added later (to give 4c). **4g** is from a streptavidin-Cy5 control experiment, in which no YOYO-control deemed necessary.

Figure 4 shows a few single-frame samples, each frame out of a movie of typically 500 to 2000 frames. 4a is from an origami experiment, with 4b being the YOYO control, showing a high coverage of origami sheets. The white spots are (assumed to be) single pVIc-Cy3b molecules, which I will further refer to as fluorescent spots or spots. 4d and 7e show the same thing for a negative control experiment. Interestingly it shows the same pVIc behaviour although no origami is

present. This tells us that pVIc is not only binding to origami, but also to the glass coverslip. 4g shows a streptavidin-Cy5 experiment. 4c and 4f are from a separate experiment controlling the difference between no origami (4f) and origami (4c) being present in the flow channel, in order to confirm the results of 4b and 4e respectively.

Trajectory plots and MSD curves

After plotting all the MSD points against their respective time frame, we arrived at hundreds of MSD curves for each movie analysed. Even after filtering out around 80% of the trajectories by choosing only trajectories with a length between 20 and 499 frames (one frame equals 16,01ms). None of the MSD curves had the characteristic confined diffusion behaviour that we were looking for.

Trying to estimate the speeds and distances of diffusion of pVIc on DNA, we arrived at the results shown in Table 1. It shows the *displacement* that pVIc can diffuse for typical *exposure times* and the *time* that it takes for pVIc to diffuse over the *characteristic lengths* of the origami sheet. These values are obtained by using equation 1 and the one dimensional diffusion coefficient of pVIc that was published by Mangel et al. [4]. Important to note is that this equation does not take into account the specific structure of the origami sheet and the specific sliding mechanism that pVIc might have and assumes that there is no directional bias in its diffusive behaviour.

Time (ms)	30,53	16,01	4,21		2,11	0,23	0,0094
Displacement (nm)	570,2	412,9	211,7		150	50	10

Table 1. **The expected displacement and diffusion time of a particle in two dimensions.** Where the first row gives the time of diffusion and the second row the displacement (square root of MSD). Equation 1, for isotropic two dimensional diffusion, and the one dimensional diffusion coefficient of pVIc, D = 2,66(um^2/s) [4], have been used to calculate these values.

These results show that it is unlikely to obtain the MSD curve that we would like to find when using a 16,01ms exposure time, because exposure times of ~10µs would be necessary to trace the path of pVIc with sufficient resolution. We tried to reduce the exposure time, but going below 4,21ms is already a challenge due to the small FOV, the lower signal to noise ratio at lower exposure time and the shorter fluorophore life at higher laser intensity. Furthermore, the camera that we were using has a minimum exposure time of 2,4ms, far above the wanted exposure time.

Another challenge is that we use 50nm x 150nm origami sheets, which makes distinguishing between sliding pVIc molecules (on DNA) and stuck pVIc molecules (on the coverslip or on DNA) difficult with a pixel size of 160nm x 160nm! In one dimensional random walk experiments that use 48k-base-pair DNA molecules (~16300nm long) we can *see* the physical displacement of pVIc along DNA, which allows for clear distinction.

While pursuing to solve the high exposure time problem, which was not solved due to an apparent oscillation of the FOV (explained in appendix B), we turned towards another problem in the meantime: using the data that we already had in order to learn something about the interaction of pVIc with DNA-origami, and to learn something about DNA-origami itself. This attempt is summarised in the following analyses.

FWHM histograms of the spot intensity distributions

It is expected that a histograms of the spot FWHM will show at least two peaks for the origami experiments, where each peak resembles a population of molecules that have distinct spatial distributions. The results do not show this behaviour, as can be seen in figure 5a and 6a: only one individual peak can be seen.

Figure 5 shows the histograms of *all FWHM* values obtained from analysing all individual fluorescent spots in all individual movie frames that belong to a 20 – 499 frame trajectory (filtering the particles according to their sliding lifetime only affects the counts of the histograms and not their form (see figure A.2 and A.3)).

Figure 6 shows the *mean FWHM* values that are calculated over each trajectory that has a sliding lifetime between 20 and 499 frames long.

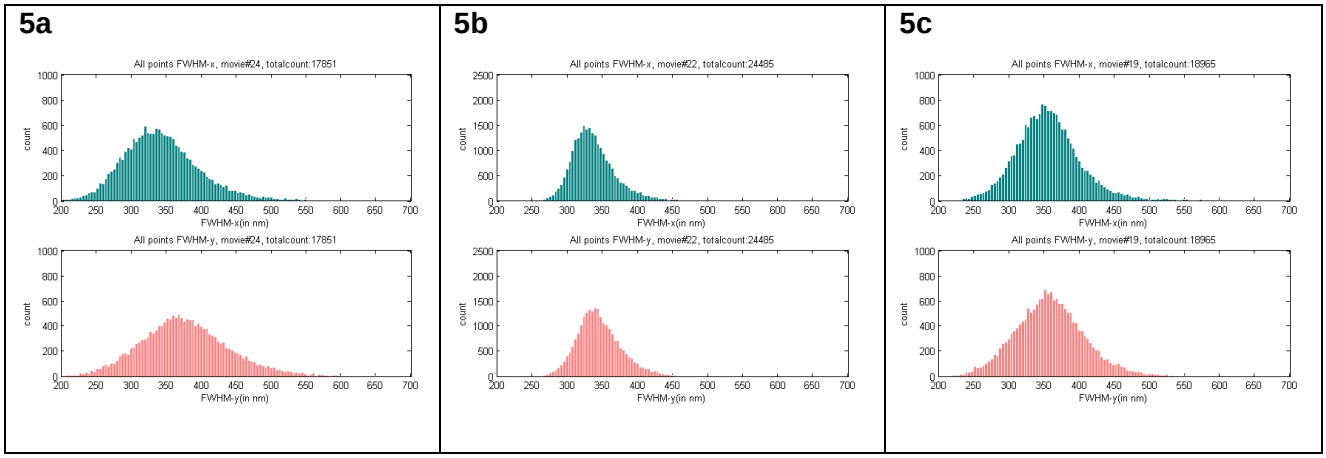

Figure 5. **Histograms of *all FWHM* values, in disrespect of their trajectory.** Origami (5a) negative control (5b) and Streptavidin-Cy5 control (5c) are shown with FWHM of the x-direction and y-direction spot intensity distribution above and below respectively. The selection parameters used in Particle Tracker are max. step size = 2, max. slice difference = 2. The data is filtered (contains all particles that are part of a 20 – 499 frame long trajectory).

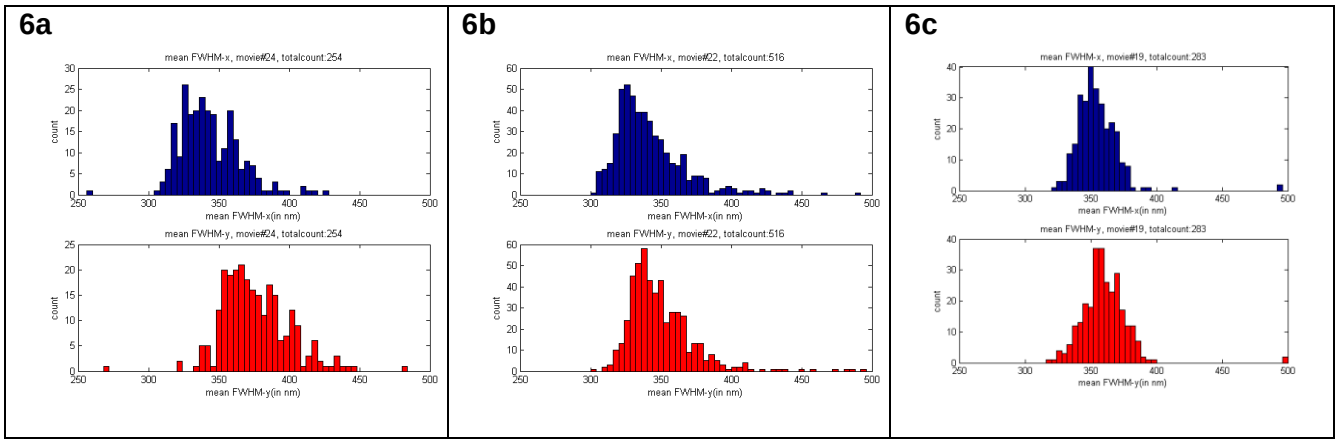

Figure 6. **Histograms of *mean FWHM* values calculated per trajectory.** Origami (6a) negative control (6b) and Streptavidin-Cy5 control (6c) are shown with FWHM of the x-direction and y-direction spot intensity distribution above and below respectively. The selection parameters used in Particle Tracker are max. step size = 2, max. slice difference = 2. The data is filtered (only trajectories lifetimes that are between 20 and 499 frames long).

We analysed the effect on the histogram when averaging the FWHM value over each trajectory that has a lifetime of 20 to 499 frames (figure 6). We are interested only in longer pVIc sliding lifetimes because it is likely to be the case for pVIc when bound to origami, considering that its "mother", pVI, has such a high binding affinity to DNA [5]. Hereby neglecting DNA-origami structural differences to normal DNA. Histograms of the mean FWHM per trajectory might add information and could distinct between two different populations of particles more clearly compared to using all FWHM values. What can be seen in figure 6 and appendix A, is that there are contours arising in the mean FWHM histograms, but this is not easy to judge with such a low number of total counts. It should also be noted that this averaging method could be susceptible to the way that trajectories are assembled.

We looked at this effect only partly (appendix A, figure A.2 – A.6) and cannot judge how strong the different selection parameters in the Particle Tracker plugin do influence the analysis.

The effect of filtering trajectories according to their lifetime does not influence the histograms of all FWHM values (see appendix A, figure A.2 and A.3). This has not been controlled for the histograms of the mean FWHM.

The presence of "active" flow (5µL/min) inside the flow channel seems to increase the relative amount of large FWHM spots (appendix A figure A.4 compared to A.5 and figure A.6 compared to A.7) This could be a coincident arising from the fact that one of the movies analysed in figure A.6 and A.7 is slightly more out of focus than the others, or it is due to the flow that causes fluctuation of the molecule at the coverslip surface [10]. "Active flow" suggests that the presence of flow cannot precisely be determined, only the state of the syringe pump is definite; this is due to the longer lasting pressure difference through the presence of an air spring, especially observable at low flow rate.

There are two more important observations that we will only touch briefly. Firstly, that there is an apparent width difference, especially between origami and negative control experiments (figure 5a and 5b). This is not so strongly resembled in the mean FWHM histograms. We attribute the main contribution of this to the differing laser intensity (different OD settings) between all the origami and negative control movies used in our analyses. Secondly the relative shift between the mean of the x-direction FWHM histogram (blue) and the mean of the y-direction FWHM histogram (red) are observed to have a larger shift in all the origami experiments (figure 5a and 6a) compared to the relative shifts in the negative control and the streptavidin-Cy5 control experiments. Does this mean that the FOV oscillations (discussed in Appendix B) only affects the origami experiment and not the others? To answer this, further experiments are necessary.

Trajectory lifetime distributions

It is also expected that we see distinct populations when looking at the trajectory lifetimes, as described in the Theory section. The lifetime histogram counts (figure 7) were plotted in separate graphs (solid lines in figure 8 and 9). These are fitted with double and single exponentials (figure 8 and 9: dashed and orange-dotted lines respectively). We also graphed these lifetime distributions with single logarithmic axes (figure 10 and 11).

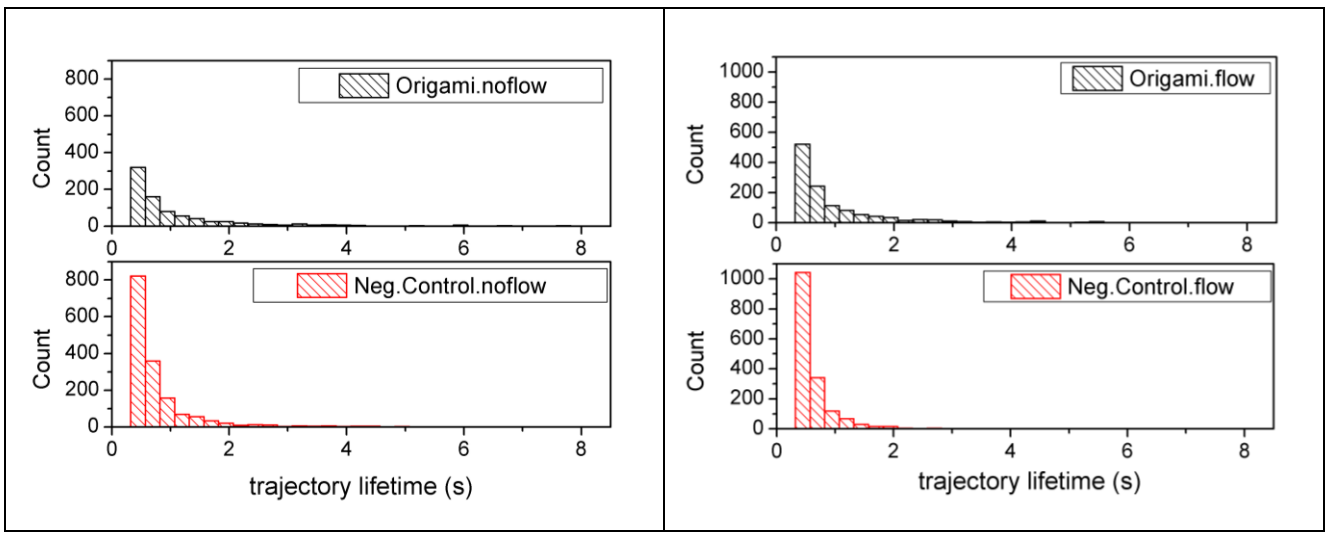

Figure 7. **Histograms of the trajectory lifetimes.** Data is collected from two or three separate movies for every histogram shown. Left are the origami (black) and negative control (red) data with no active flow (~0 µL/min) through the flow channel. On the right the same for movies where the syringe pump is set to 5 µL/min.

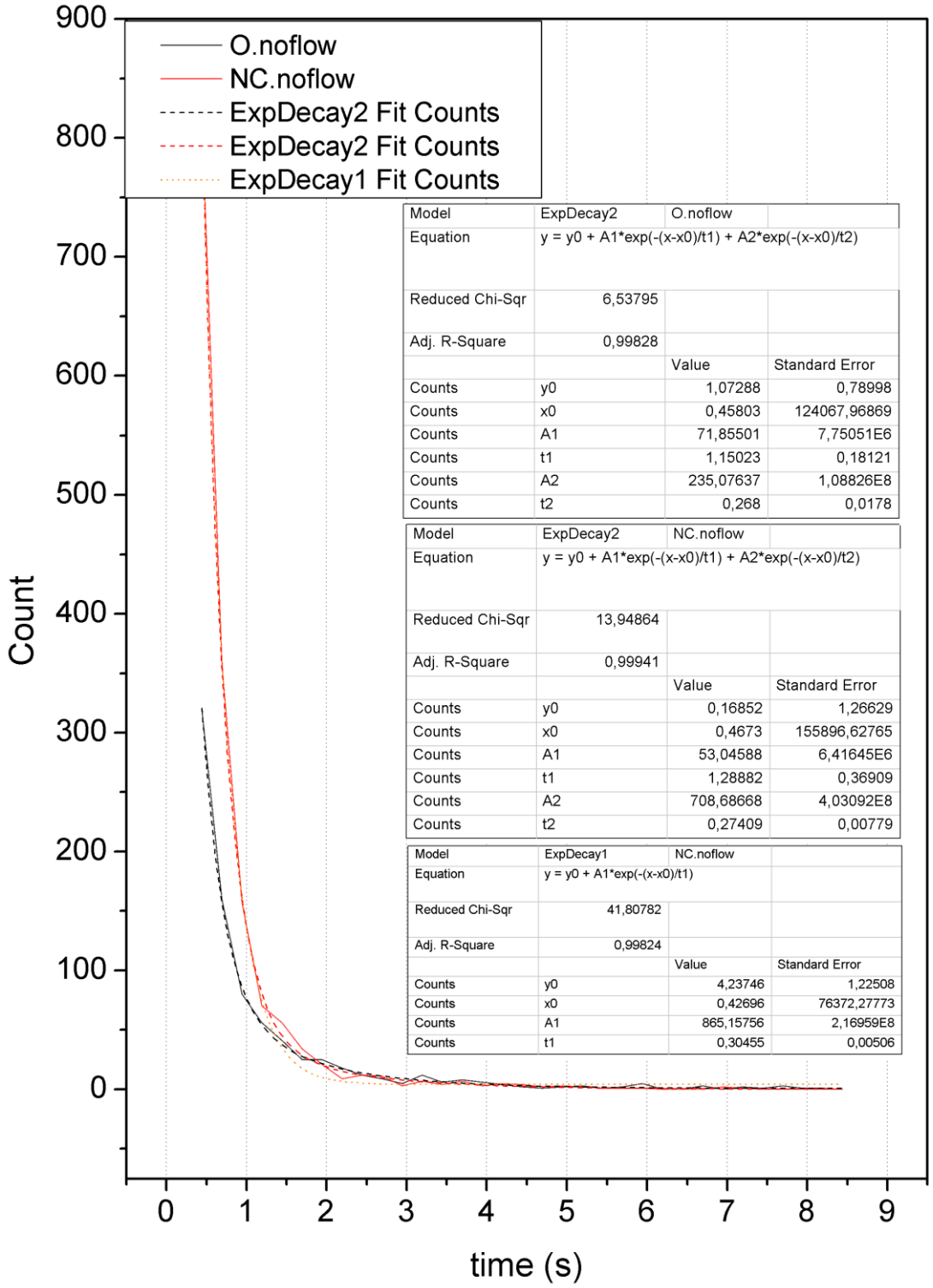

Model	ExpDecay2	O.noflow	
Equation	y = y0 + A1*exp(-(x-x0)/t1) + A2*exp(-(x-x0)/t2)		
Reduced Chi-Sqr	6,53795		
Adj. R-Square	0,99828		
		Value	Standard Error
Counts	y0	1,07288	0,78998
Counts	x0	0,45803	124067,96869
Counts	A1	71,85501	7,75051E6
Counts	t1	1,15023	0,18121
Counts	A2	235,07637	1,08826E8
Counts	t2	0,268	0,0178

Model	ExpDecay2	NC.noflow	
Equation	y = y0 + A1*exp(-(x-x0)/t1) + A2*exp(-(x-x0)/t2)		
Reduced Chi-Sqr	13,94864		
Adj. R-Square	0,99941		
		Value	Standard Error
Counts	y0	0,16852	1,26629
Counts	x0	0,4673	155896,62765
Counts	A1	53,04588	6,41645E6
Counts	t1	1,28882	0,36909
Counts	A2	708,68668	4,03092E8
Counts	t2	0,27409	0,00779

Model	ExpDecay1	NC.noflow	
Equation	y = y0 + A1*exp(-(x-x0)/t1)		
Reduced Chi-Sqr	41,80782		
Adj. R-Square	0,99824		
		Value	Standard Error
Counts	y0	4,23746	1,22508
Counts	x0	0,42696	76372,27773
Counts	A1	865,15756	2,16959E8
Counts	t1	0,30455	0,00506

Figure 8. **Lifetime distributions for no active flow (~0 µL/min)**. Showing lifetime distributions derived from plotting the histograms' count values (from figure 7) as solid lines. With origami experiment in black and negative control in red (and orange). The double exponential and single exponential fits of the distributions are shown as dashed and dotted lines respectively. The fit parameters are shown in the tables in the graph, labelled accordingly.

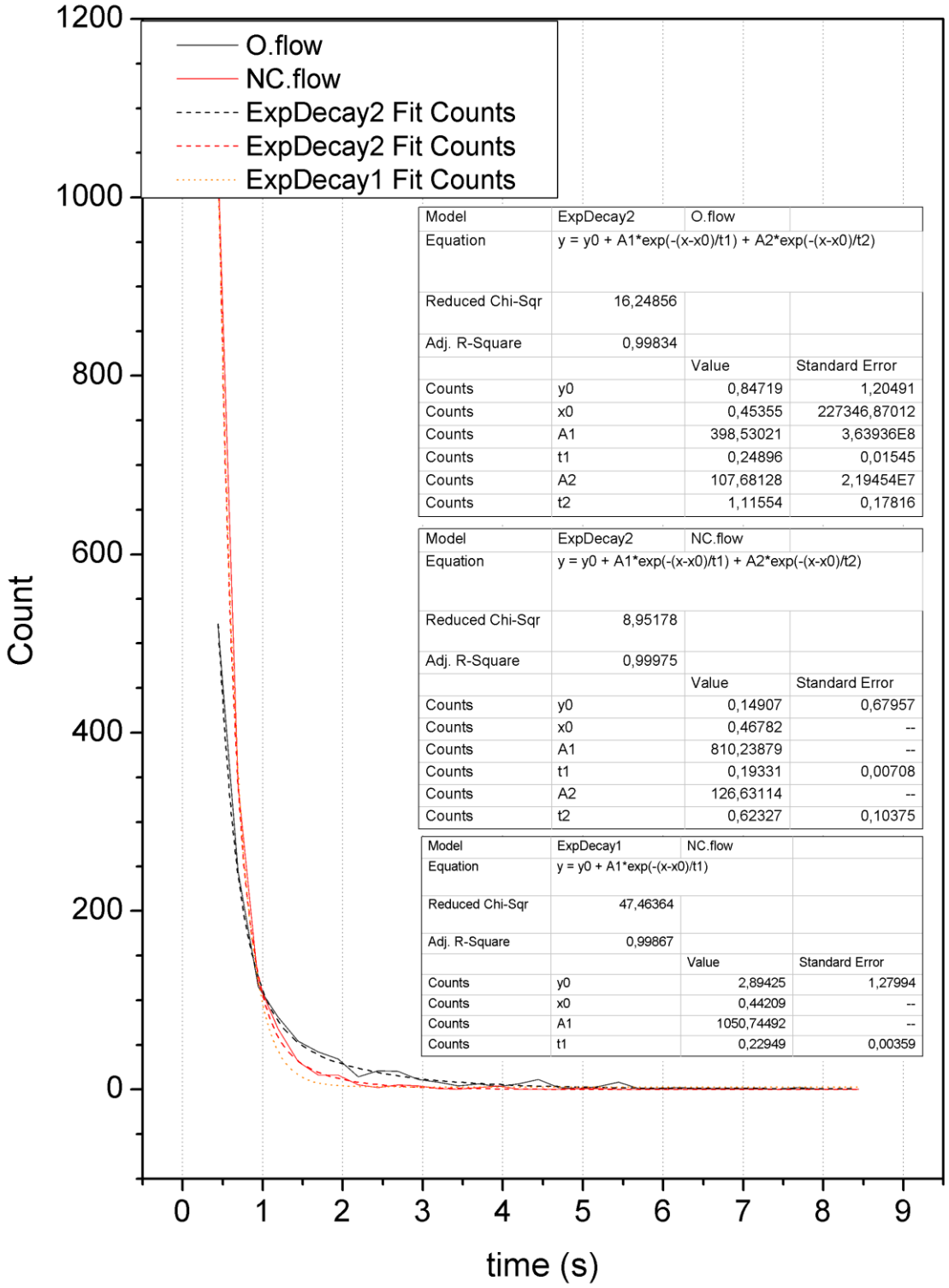

Model	ExpDecay2	O.flow	
Equation	y = y0 + A1*exp(-(x-x0)/t1) + A2*exp(-(x-x0)/t2)		
Reduced Chi-Sqr	16,24856		
Adj. R-Square	0,99834		
		Value	Standard Error
Counts	y0	0,84719	1,20491
Counts	x0	0,45355	227346,87012
Counts	A1	398,53021	3,63936E8
Counts	t1	0,24896	0,01545
Counts	A2	107,68128	2,19454E7
Counts	t2	1,11554	0,17816

Model	ExpDecay2	NC.flow	
Equation	y = y0 + A1*exp(-(x-x0)/t1) + A2*exp(-(x-x0)/t2)		
Reduced Chi-Sqr	8,95178		
Adj. R-Square	0,99975		
		Value	Standard Error
Counts	y0	0,14907	0,67957
Counts	x0	0,46782	--
Counts	A1	810,23879	--
Counts	t1	0,19331	0,00708
Counts	A2	126,63114	--
Counts	t2	0,62327	0,10375

Model	ExpDecay1	NC.flow	
Equation	y = y0 + A1*exp(-(x-x0)/t1)		
Reduced Chi-Sqr	47,46364		
Adj. R-Square	0,99867		
		Value	Standard Error
Counts	y0	2,89425	1,27994
Counts	x0	0,44209	--
Counts	A1	1050,74492	--
Counts	t1	0,22949	0,00359

Figure 9. **Lifetime distributions for active flow (5 µL/min)**. Showing lifetime distributions derived from plotting the histograms' count values (from figure 7) as solid lines. With origami experiment in black and negative control in red (and orange). The double exponential and single exponential fits of the distributions are shown as dashed and dotted lines respectively. The fit parameters are shown in the tables in the graph, labelled accordingly.

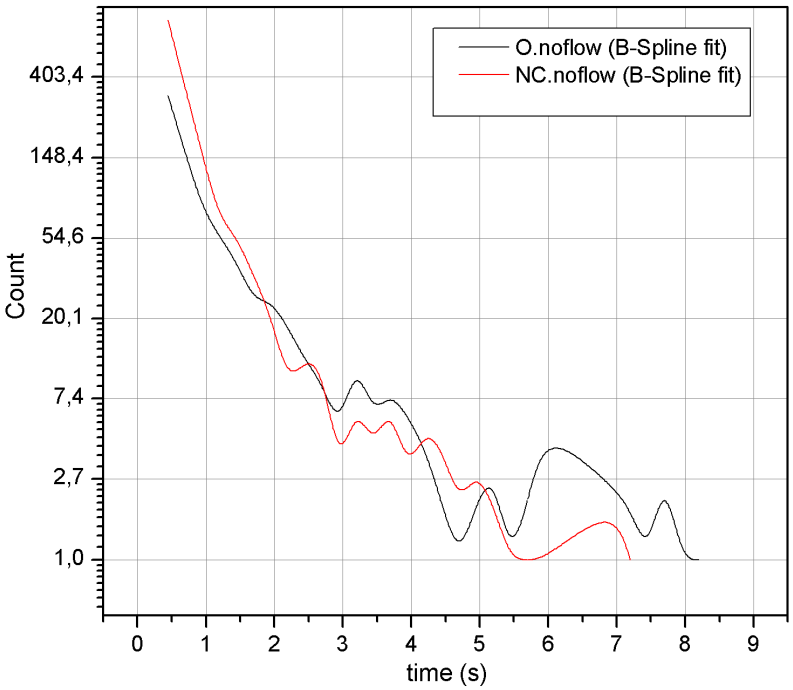

Figure 10. L**ifetime distributions plotted with single-logarithmic scale (~0 µL/min)**. The origami experimental data is shown in black and negative control in red. The points are connected with a B-Spline fit, for better clarity.

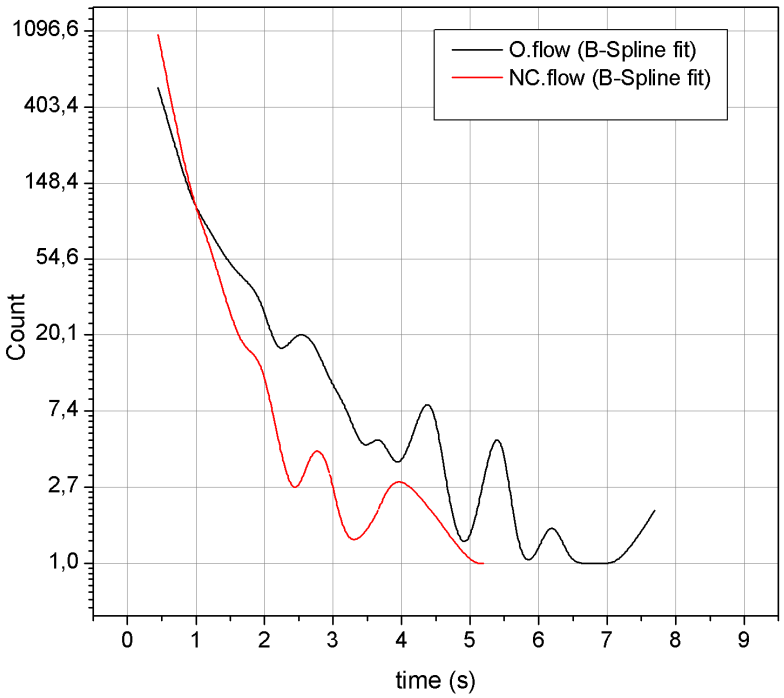

Figure 11. L**ifetime distributions plotted with single-logarithmic scale (5 µL/min)**. The origami experimental data is shown in black and negative control in red. The points are connected with a B-Spline fit, for better clarity.

These results correspond more closely with our predictions than the FWHM study that we did. The negative control (red line) tends to be more steeply falling off and thus looks like having a greater tendency towards single exponential decay than the origami experiment (black line). This can also be seen when looking at the histograms (figure 7). But when we compare the time constants given in the tables alongside figure 8 and 9, there is no clear tendency to be seen. They all show two differing time constants t1 and t2. This makes the single exponential decay (orange-dotted lines) trivial, but it might come in as a good reference.

Between no active flow (figure 8) and flow (figure 9) there is no relevant difference to be noted, they both show similar character. This cannot be said for the single logarithmic graphs however (figure 10 and 11). They show a clear difference for the case when there is flow present. In fact there is not much new to be learnt. This is an example of how different methods of displaying data can highlight certain details differently. There seem to be some differences in slope, but we do not see the expected double slope for the origami experiment and single slope for the negative control. This does not allow us to make clear estimates of the gradient without subjectively influencing the linear fit (see appendix A for an attempt to characterise some gradients).

It should be noted that once again, the differing laser intensity between origami and negative control experiments are likely to be the cause of the differing lifetime distributions due to its influence on fluorophore bleaching!

Similarly as already done for the FWHM analysis, we also analysed the effect of trajectory selection parameters of the Particle Tracker plugin. This time we varied only one selection parameter at a time. The complete set of graphs can be seen in Appendix A, there is no notable difference when changing the selection parameters only a little bit.

Mean FWHM versus lifetime plots

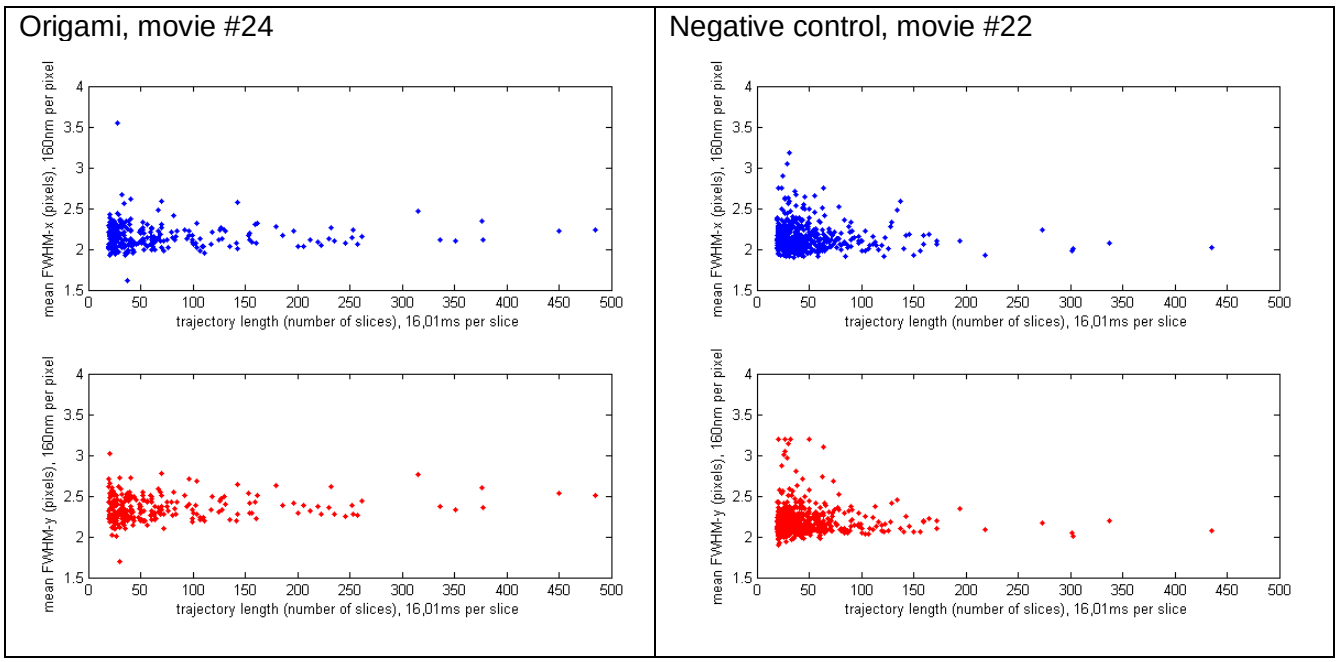

Figure 12. **Scatter plots of trajectory mean FWHM plotted as a function of trajectory lifetime**. On the left hand side is one selection out of the origami experiment movies and on the right hand side one out of the negative control experiment movies. Above (blue) and below (red) are the x-direction (flow direction) and y-direction FWHM values respectively.

Plotting the mean FWHM as function of lifetime for every trajectory (figure 12) was done as an attempt to identify whether trajectories with a short lifetime (possibly those that are sticking to the coverslip glass) have a specific tendency for broader or narrower FWHM when comparing them to

the trajectories with a longer lifetime. The results unanimously show the same relation between mean FWHM and lifetime, which is constant at around mean FWHM = 2,1pixels = 336nm. For the origami experiment y-direction (red graph) this value lies at around 2,4pixels = 384nm due to the FOV oscillations. In fact, the mean FWHM as function of lifetime graphs are nothing else than the mean FWHM histograms, but now distributed along a third parameter: the trajectory lifetime (x-axes in figure 12).

MSD plateaus

Another way to obtain information from the data that we had was by looking at the value of the MSD at which the MSD curve is flattening off to a horizontal (further referred to as *plateau value*), which tell us the typical size of the confinement. For the used origami sheets this corresponds to 50nm*150nm = 7500nm^2 = 0,0075µm^2. Figure 13 shows the beginning of a histogram of these plateau values (in µm^2). Note that this is more a proof of principle than an analysis from which conclusions can be made because data is insufficient and approximate (no error margin known).

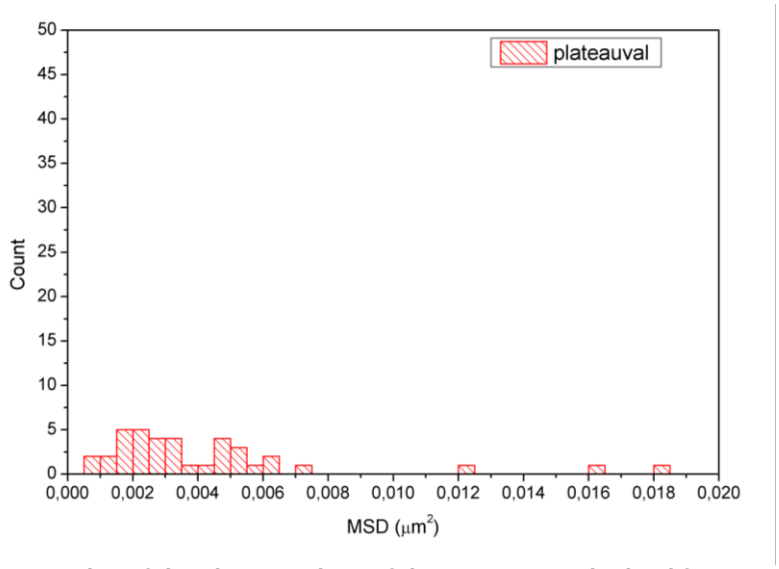

Figure 13. **Histogram of MSD value of the plateau values of the MSD curve obtained for one origami experiment**. Note: this is only a proof of principle, data is very approximate.

What we can see is that most of them lie below the expected value. This suggests that there are hardly any molecules bound to origami, or that they are not sliding on origami. Interestingly, the roughly estimated accuracy of our centroid positions is 50nm*50nm = 0,0025µm^2.

But before we can state anything, we need to collect more data and develop a more robust method to determine the correct plateau value with error margin. This is not always straight forward, especially for short trajectories with a lot of fluctuation. The data used for this analysis is from one origami experiment only.

My Conclusion and Perspective

In the light of the many analyses done in this Bachelor project I finish off with a lot of breadth and rather little focus on one question. Wanting to unravel the behaviour of pVIc on DNA-origami, many unknowns were facing me from the start, but a start had to be made somewhere. Therefore questions are left unaddressed and unanswered, but a few things can be said which will mainly contribute to the success of following experiments.

The long exposure time of the camera prevented me from obtaining the MSD curve of interest. I have thought about using short laser pulses which reduce the window in which we observe kinetic information of the molecule, but this would not give us the wanted MSD curve. This is because the particle displacement from one pulse to the next still depends on the time *between* the pulses and thus again on the camera exposure time, unless we can distinct several pulses within one timeframe. What shorter pulses would give us though is a more accurate picture of the molecule position due to the smaller spatial distribution (see equation 3).

The position accuracy, which is close to the characteristic size of the origami sheet itself, probably also contributed to the fact that different particle populations were not distinguishable in the FWHM analysis. This is because the FWHM analysis is based on the spatial distribution which was in this case very similar to the accuracy.

I believe that the expected differences that I observe in both the FWHM and the trajectory lifetime analysis are mainly induced by the differing laser intensities between origami and negative control experiments!

A lesser problem, but indeed notable, are the different Particle tracker settings. They were not large enough to see a change in the analyses I made in Appendix A, but I definitely observed that long trajectories are often recorded as several short trajectories (from comparing the length of trajectories with the actual particle movies).

FWHM analyses have left us only with the question to pursue whether the FOV oscillations (appendix B) affect only the origami experiment, or also the other experiments? To answer this it is necessary to acquire low exposure time movies of negative control and maybe Streptavidin-Cy5 control experiments.

For looking at the effects that Particle Tracker has on the results, the same analyses need to be done with equal laser intensity and larger increases of the max. slice difference selection parameter (some more than I already increased it). Looking at other parameters of the Particle Tracker plugin is maybe also an option. This also comes with the risks of accidentally observing different, shorter trajectories as one single long trajectory.

If we know for sure that the origami sheet pattern is really a set of helices stacked next to one another, it might be interesting to use larger origami sheets and study whether pVIc has a preference for sliding along the double helix grain of the origami sheet. Assuming that pVIc slides on origami at all. This only leaves us with the challenge of appropriately fixing and positioning larger origami structures. Other DNA-origami structures are also an option (like for instance origami tubes that can be stretched by flow through the channel.

Apart from the FOV oscillation problem that should be solved, further increase of the accuracy is possible by reducing the noise and maximising flurophore intensity, but that is not very easy due to technical and chemical limitations.

The MSD plateau value histograms could give a good picture if more data is collected in a reliable manner.

My closing statement is that I have learnt that it is wise to think carefully about how prior knowledge can teach me about what kind of outcomes I can expect. Even so, it was still worthwhile to try this specific experiment, due to many unknowns that could have given me some unexpected results… and who knows, maybe I just did not see these results yet.

References

1. Anahita Tafvizi, Leonid A. Mirny, and Antoine M. van Oijen (**10 May 2011**), *Dancing on DNA: Kinetic Aspects of Search Processes on DNA*, ChemPhysChem 2011, 12, 1481-1489.

2. Paul C. Blainey, Antoine M. van Oijen, Anirban Banerjee, Gregory L. Verdine, and X. Sunney Xie (**11 April 2006**), *A base-excision DNA-repair protein finds intrahelical lesion bases by fast sliding in contact with DNA*, PNAS Vol. 103, No. 15, pp. 5752-5757.

3. Anahita Tafvizi, Fang Huang, Jason S. Leith, Alan R. Fersht, Leonid A. Mirny, and Antoine M. van Oijen (**8 April 2008**), *Tumor Suppressor p53 Slides on DNA with Low Friction and High Stability*, Biophysical Journal: Biophysical Letters.

4. Vito Graziano, Guobin Luo, Paul C. Blainey, Ana J. Pérez-Berná, William J. McGrath, S. Jane Flint, Carmen San Martín, X. Sunney Xie, and Walter F. Mangel (**2012**)*, Regulation of a Viral Proteinase by a Peptide and DNA in One-dimensional Space: II. ADENOVIRUS PROTEINASE IS ACTIVATED IN AN UNUSUAL ONE-DIMENSIONAL BIOCHEMICAL REACTION*, J. Biol. Chem. 2013, Vol. 288, pp. 2068-2080.

5. Vito Graziano, William J. McGrath, Maarit Suomalainen, Urs F. Greber, Paul Freimuth, Paul C. Blainey, Guobin Luo, X. Sunney Xie, and Walter F. Mangel (**2012**), *Regulation of a Viral Proteinase by a Peptide and DNA in One-dimensional Space: I. BINDING TO DNA AND TO HEXON OF THE PRECURSOR TO PROTEIN VI, pVI, OF HUMAN ADENOVIRUS,* J. Biol. Chem. 2013, Vol. 288, p. 2068-2080.

6. Remarks made during the discussion after my presentation in the Single-Molecule Biophysics group meeting (**21 June 2013**). See also ref. 3 supplementary for equation on calculating accuracy of centroid position.

7. J. C. Schweizer (**26 January 2007**), *Practical Course: Single-Particle-Tracking*, Biological Center of the T.U. Dresden.

8. N. A. Tanner and A. M. van Ojien, *Chapter eleven: Visualizing DNA Replication at the Single-Molecule Level*, Methods in Enzymology, Vol. 75, pp. 259-278.

9. Paul W. K. Rothemund (**16 March 2006**), *Folding DNA to create nanoscale shapes and patterns*, Nature, Vol. 440.

10. In correspondence with the findings of Sarah Stratmann during a discussion with me (**mid June 2013**).

Appendix A: Data

MSD curves and their trajectory plots

In order to get a picture of the data and its trends, here follows a selection of MSD curves that we have picked out because they can be seen repeatedly throughout the large crowd of MSD curves (figure A.1). Note that it might not be wise to categorize the MSD-curve characteristics because there is more behind them than meets the eye.

A.1a

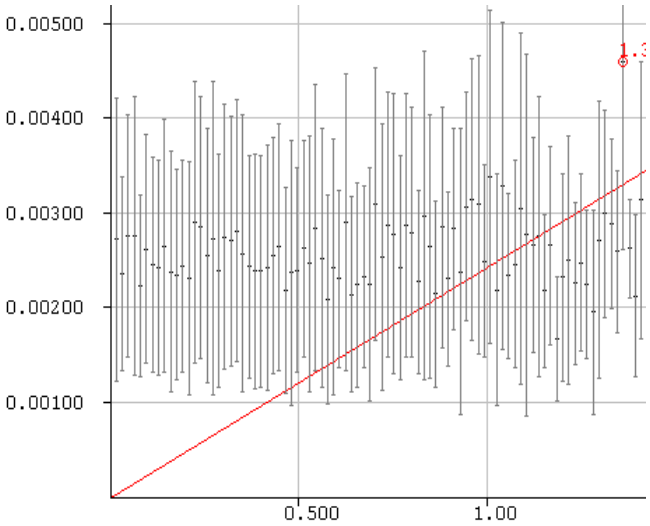

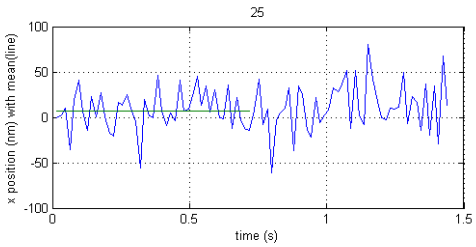

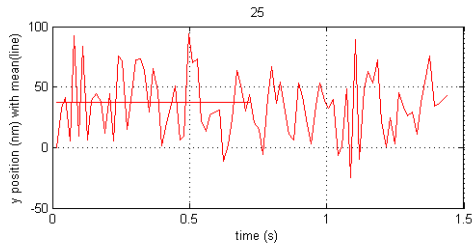

A.1b

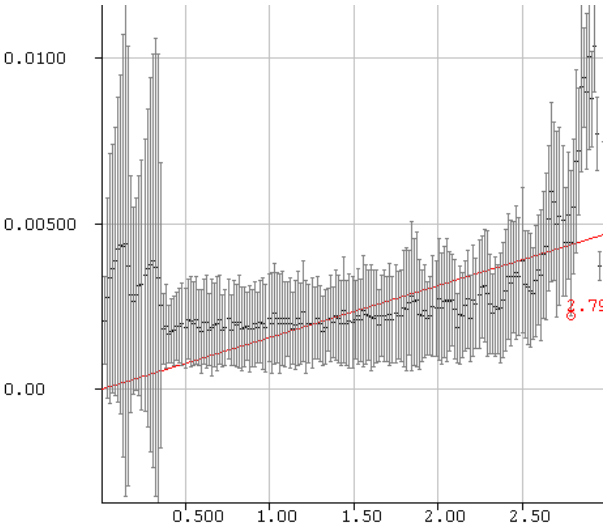

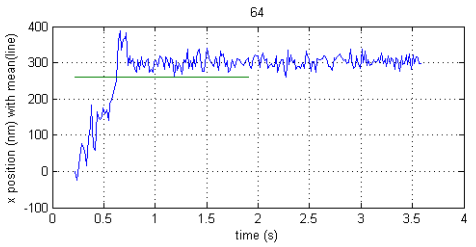

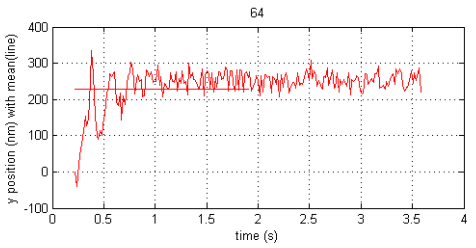

A.1c

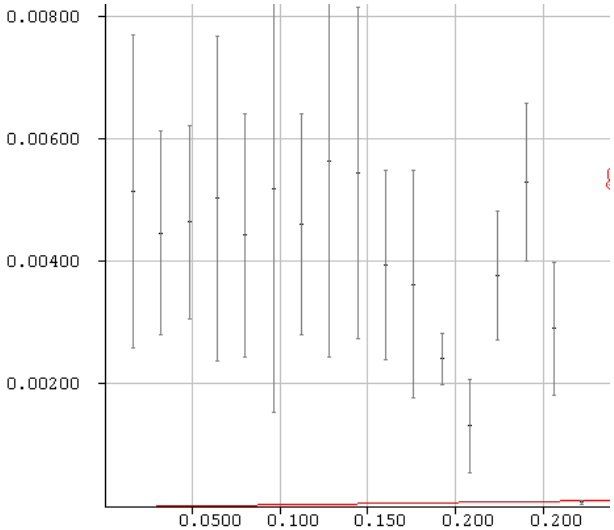

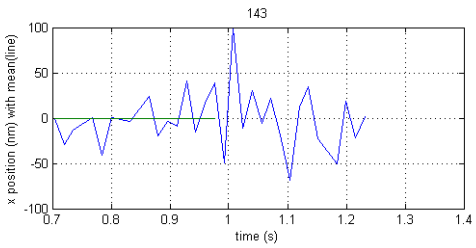

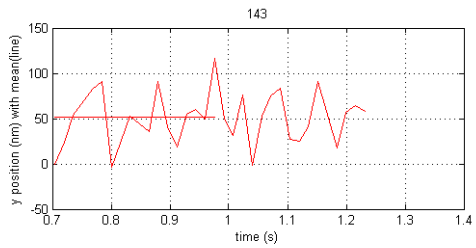

A.1d

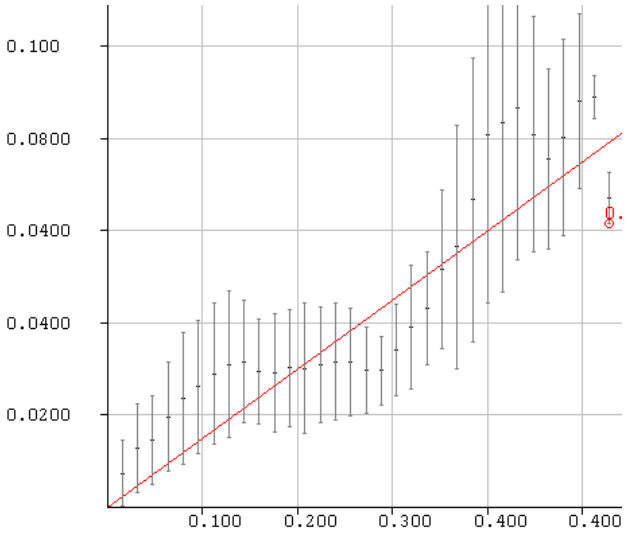
0.100
0.0800
0.0400
0.0400
0.0200
0.100
0.200
0.300
0.400
0.400

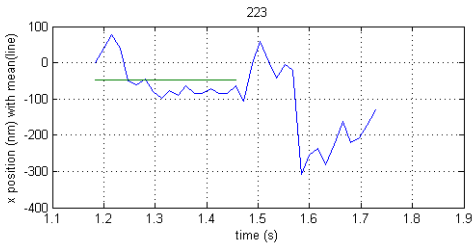
223
x position (nm) with mean(line)
time (s)

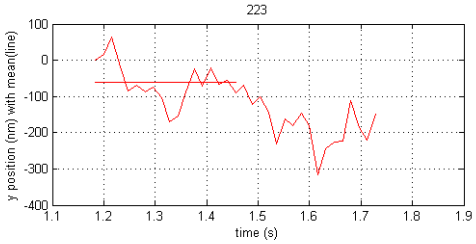
223
y position (nm) with mean(line)
time (s)

A.1e

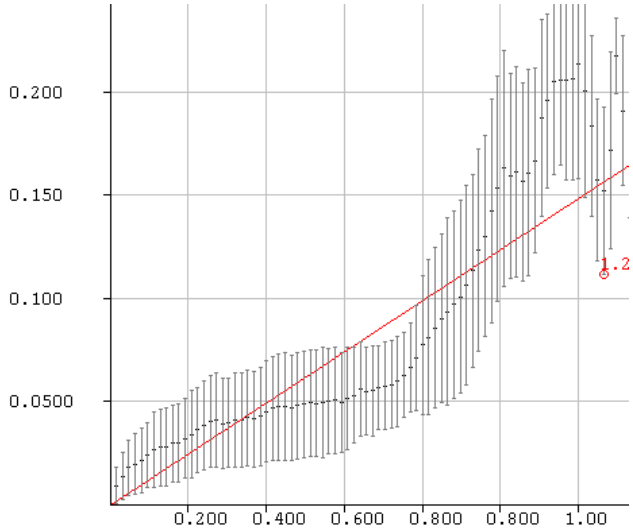
0.200
0.150
0.100
0.0500
0.200
0.400
0.600
0.800
0.800
1.00

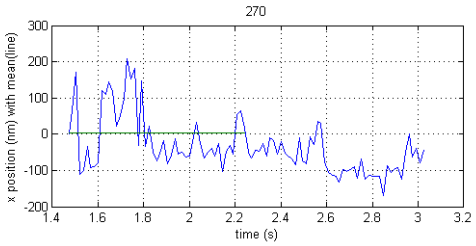
270
x position (nm) with mean(line)
time (s)

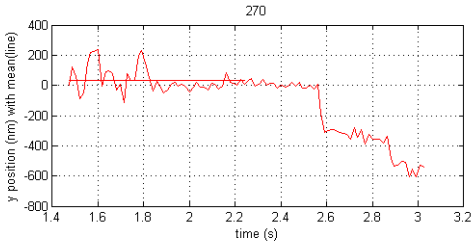
270
y position (nm) with mean(line)
time (s)

A.1f

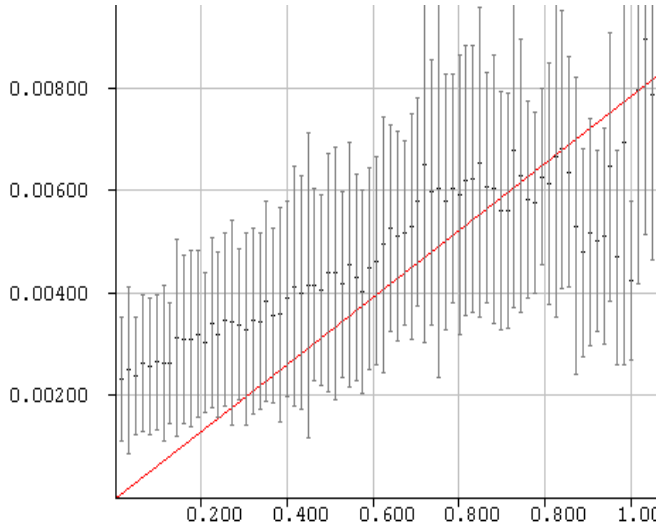
0.00800
0.00600
0.00400
0.00200
0.200
0.400
0.600
0.800
0.800

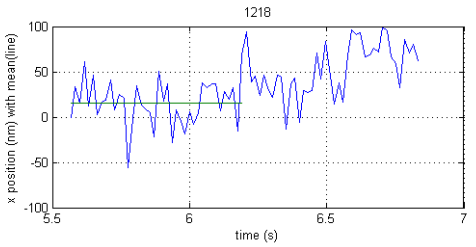
1218
x position (nm) with mean(line)
time (s)

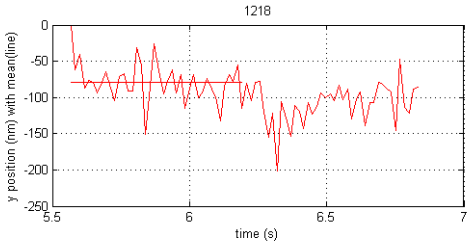
1218
y position (nm) with mean(line)
time (s)

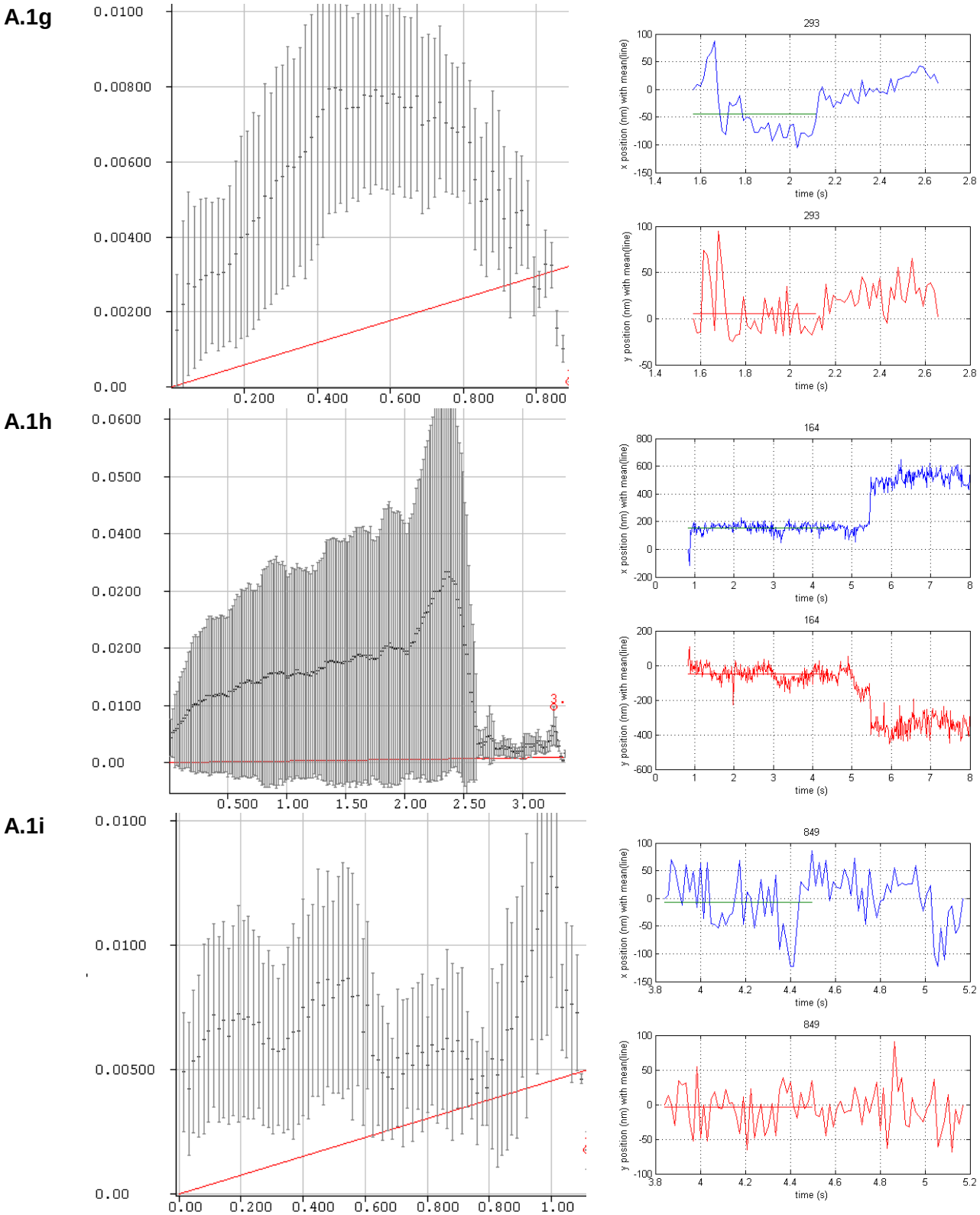

Figure A.1. **Selection of trajectories' MSD curves (left hand side) and their trajectory plots (right hand side) which were selected from movie #12 (folder 130507).** They are selected on basis of their MSD curve characteristics. MSD graph axes are: MSD (um^2) as function of time (s). Please neglect the red linear interpolation in the MSD graph, they are due to a built in function of the software and are neglected in my analyses. Trajectory graphs are given for their respective x-displacements (top, blue) and y-displacements (bottom, red) with graph axes as displacement (nm) as function of time (s). Note that the trajectory time does not start at time=0. The title is the trajectory number that is assigned to this specific trajectory.

1a-1c show the plateau behaviour that is discussed in Results and Discussion. **1d-1e** are a combination of different inclines that decide to start and end at a certain point in time. **1f** shows a uniform linear behaviour. **1g** is merely displayed because it occurs noticeably often throughout the large number of MSD curves per movie. **1h-1i** show "jumping plateaus". This possibly comes from partly confined diffusion behaviour in which the particle is moves to another position, hovering there a bit, before moving on to another position. This could arise from pVIc moving from Origami sheet to origami sheet.

The question left open here is: how do the particles behave that give me these specific curves? We have looked at some, but not all. The step from movie to MSD curve is not straight forward and it is difficult to differentiate between movies that have differing MSD curve character as is suggested in figure A.1.

The main observation when looking at these movies is that the Particle Tracker does not track the particles' entire trajectory every time.

FWHM histograms analysis

Here we show the remaining FWHM histograms of all FWHM values (figure A.2 and A.3) with no active flow and active flow, and mean FWHM values (figure A.4 – A.7) with no active flow/ active flow and differing trajectory selection parameters (Particle Tracker plugin). The movies shown in figure A.5 – A.7 are the same ones used also in the lifetime analysis (only one of them, with very low count, is not shown).

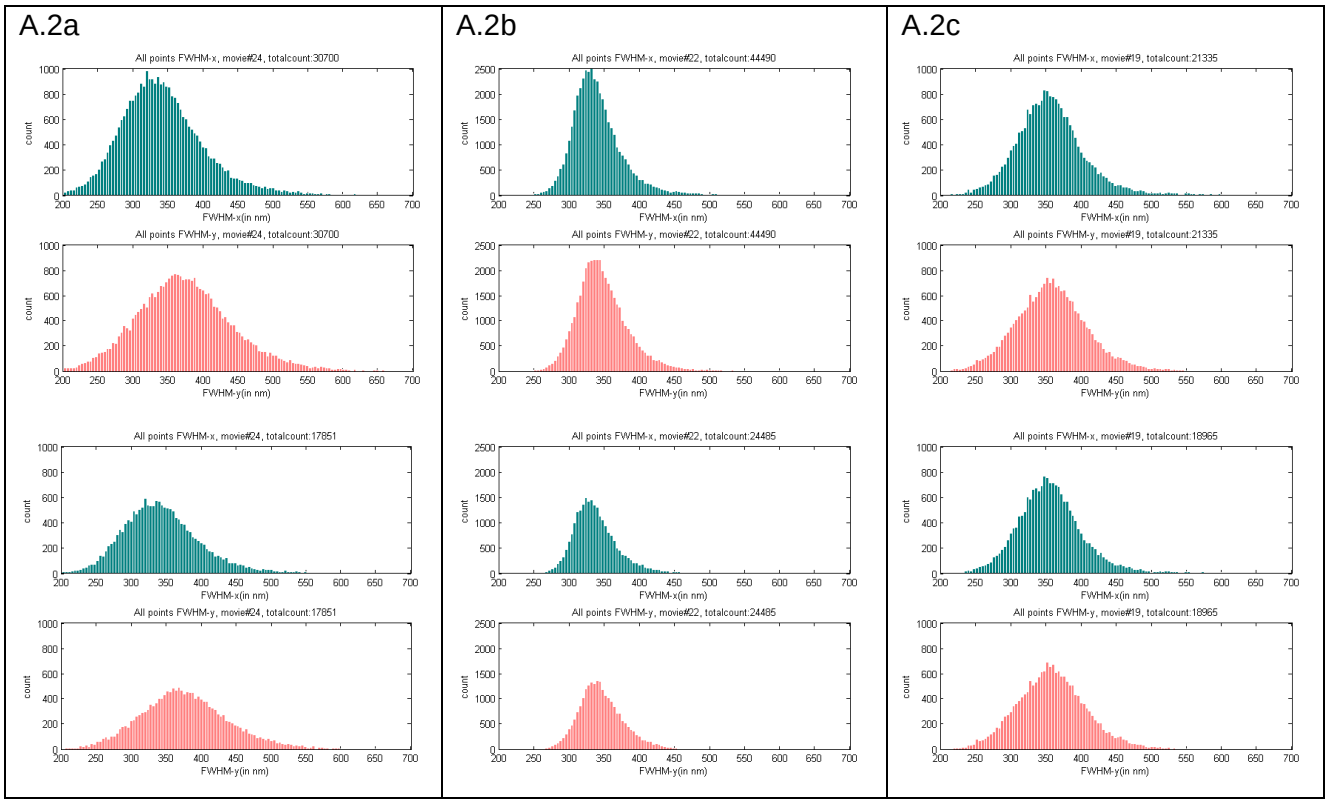

Figure A.2. **Histograms of *all FWHM* values, in disrespect of their trajectory. No flow (~0µL/min), Particle Tracker parameters:** max. step size = 2, max. slice difference = 2**.**
Origami (A.2a) negative control (A.2b) and streptavidin-Cy5 control (A.2c) are shown where the top two histograms are from unfiltered data and the bottom two histograms from filtered data (only trajectories with lifetimes between 20 and 499 frames). The FWHM of the x-direction and y-direction are shown above (blue) and below (red) respectively.

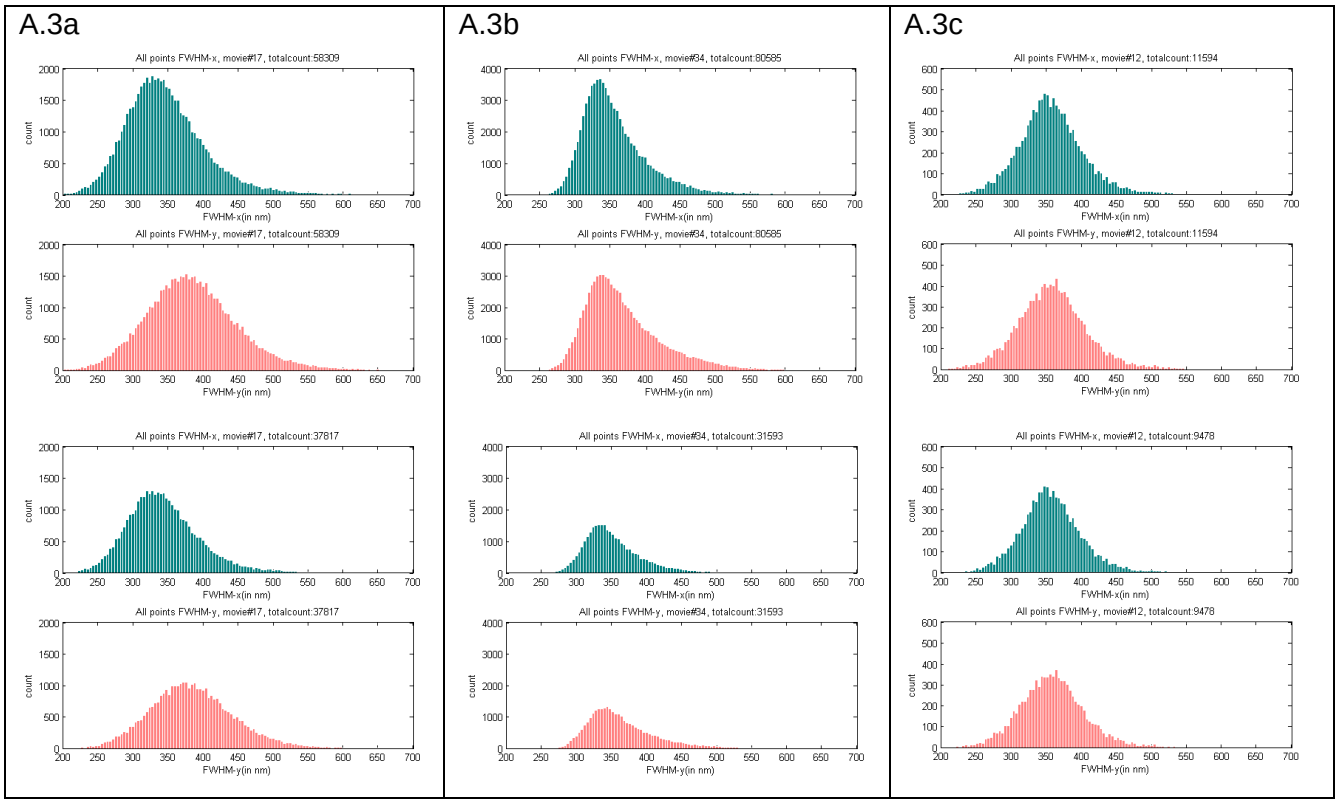

Figure A.3. **Histograms of *all FWHM* values, in disrespect of their trajectory. Flow (5µL/min, 10µL/min for Cy5 control), Particle Tracker parameters:** max. step size = 2, max. slice difference = 2**.**
Origami (A.3a) negative control (A.3b) and streptavidin-Cy5 control (A.3c) are shown where the top two histograms are from unfiltered data and the bottom two histograms from filtered data (only trajectories with lifetimes between 20 and 499 frames). The FWHM of the x-direction and y-direction are shown above (blue) and below (red) respectively.

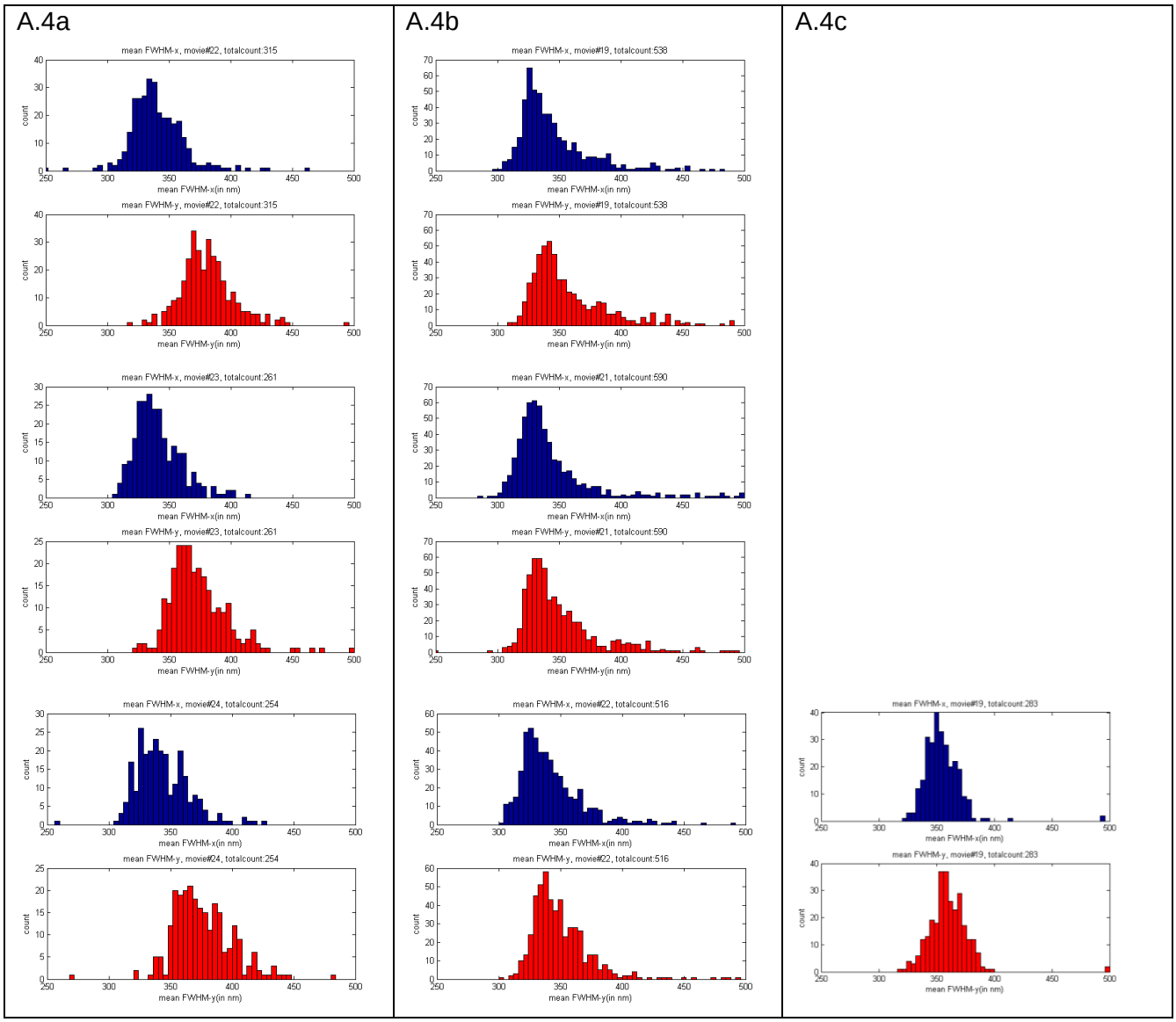

Figure A.4. **Histograms of *mean FWHM* values calculated per trajectory. No flow (~0µL/min), Particle Tracker parameters:** max. step size = 2, max. slice difference = 2**.** All data is filtered (only contains trajectories with lifetimes between 20 and 499 frames).
Three movies of Origami (A.4a) negative control (A.4b) and one movie of streptavidin-Cy5 control (A.4c) are shown. The FWHM of the x-direction and y-direction are shown above (blue) and below (red) respectively.

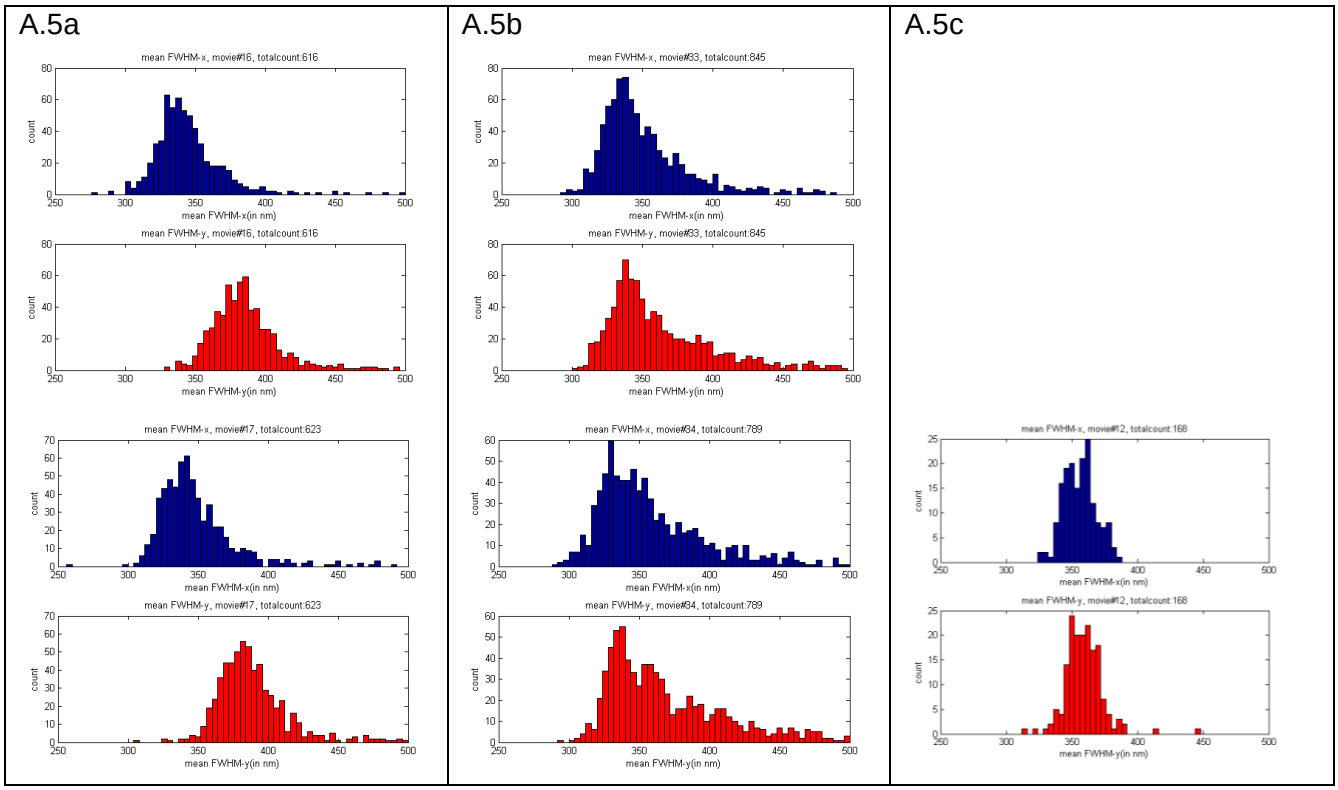

Figure A.5. **Histograms of *mean FWHM* values calculated per trajectory. Flow (5µL/min, 10µL/min for Cy5 control), Particle Tracker parameters:** max. step size = 2, max. slice difference = 2**.** All data is filtered (only contains trajectories with lifetimes between 20 and 499 frames).
Three movies of Origami (A.5a) negative control (A.5b) and one movie of streptavidin-Cy5 control (A.5c) are shown. The FWHM of the x-direction and y-direction are shown above (blue) and below (red) respectively.

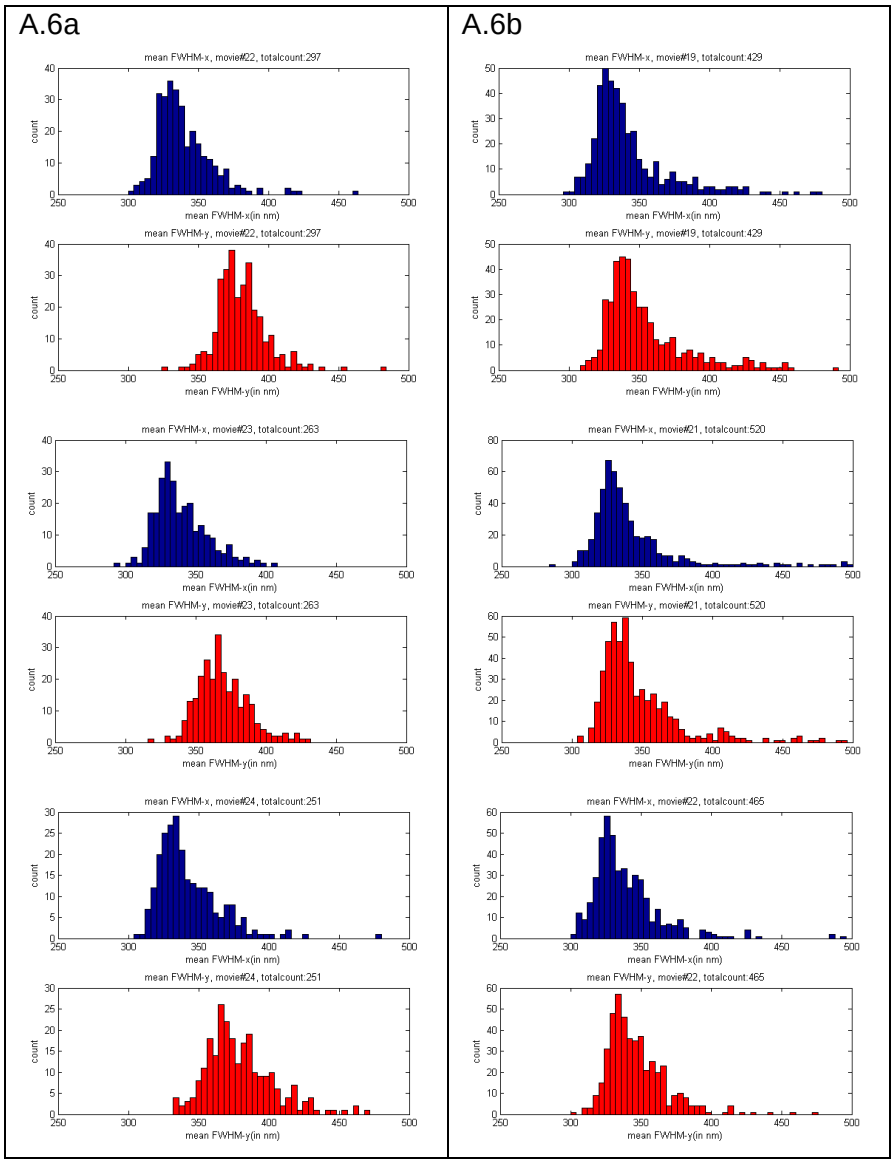

Figure A.6. **Histograms of *mean FWHM* values calculated per trajectory. No flow (~0µL/min), Particle Tracker parameters:** max. step size = 1, max. slice difference = 1**.** All data is filtered (only contains trajectories with lifetimes between 20 and 499 frames).
Three movies of Origami (A.6a) and negative control (A.6b) are shown. The FWHM of the x-direction and y-direction are shown above (blue) and below (red) respectively.

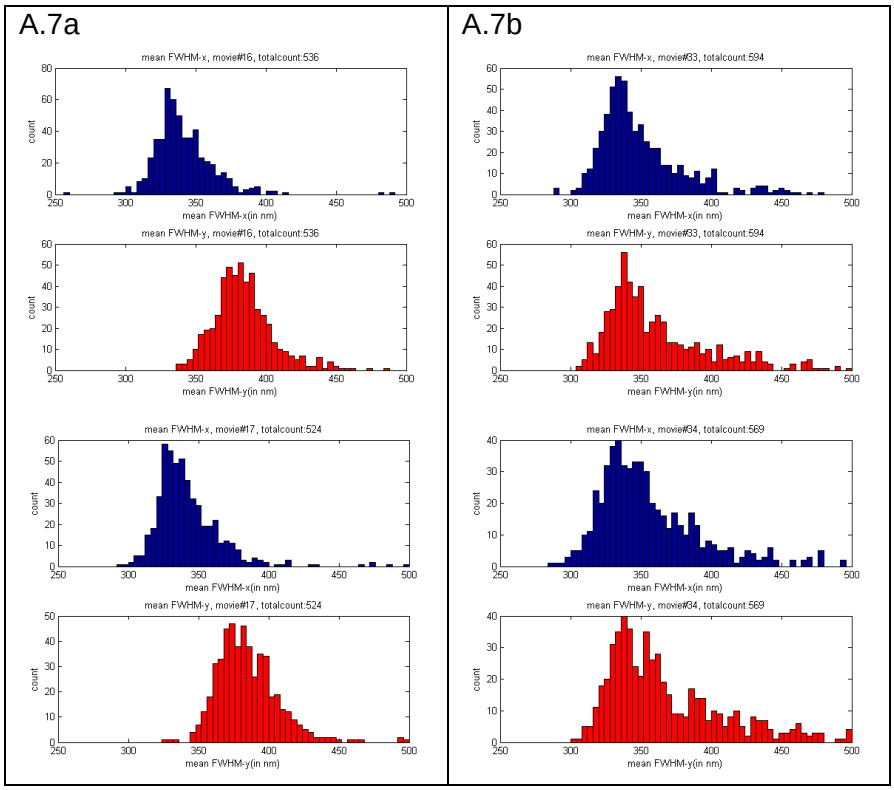

Figure A.7. **Histograms of *mean FWHM* values calculated per trajectory. Flow (5µL/min), Particle Tracker parameters:** max. step size = 1, max. slice difference = 1**.** All data is filtered (only contains trajectories with lifetimes between 20 and 499 frames).
Three movies of Origami (A.7a) negative control (A.7b) are shown. The FWHM of the x-direction and y-direction are shown above (blue) and below (red) respectively.

Trajectory lifetime analysis

Here follow the remaining trajectory lifetime distributions that show the results for varying the different selection parameters in the Particle Tracker plugin. The data used is the same for each analysis, which is also used in the mean FWHM analysis (figure A.4 – A.7).

- Particle Tracker parameters: max. step size = 2, max. slice difference = 2:

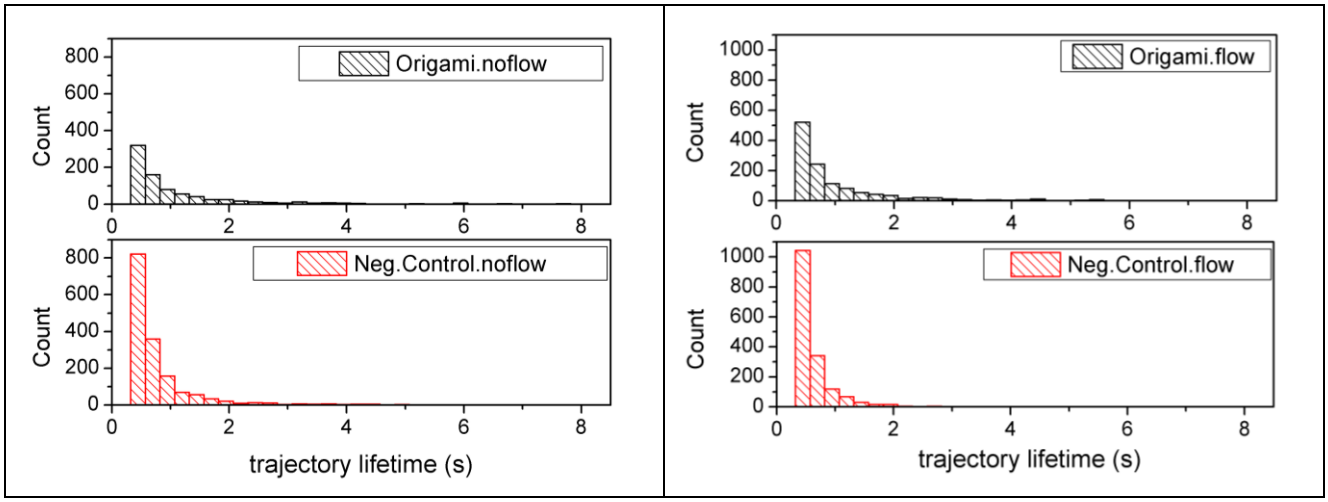

Figure A.8. **Histograms of the trajectory lifetimes, Particle Tracker parameters: max. step size = 2, max. slice difference = 2.** Data is collected from two or three separate movies for every histogram shown. On the left hand side is the origami (black) and negative control (red) data for no active flow (~0µL/min). On the right hand side the data with active flow (5µL/min).

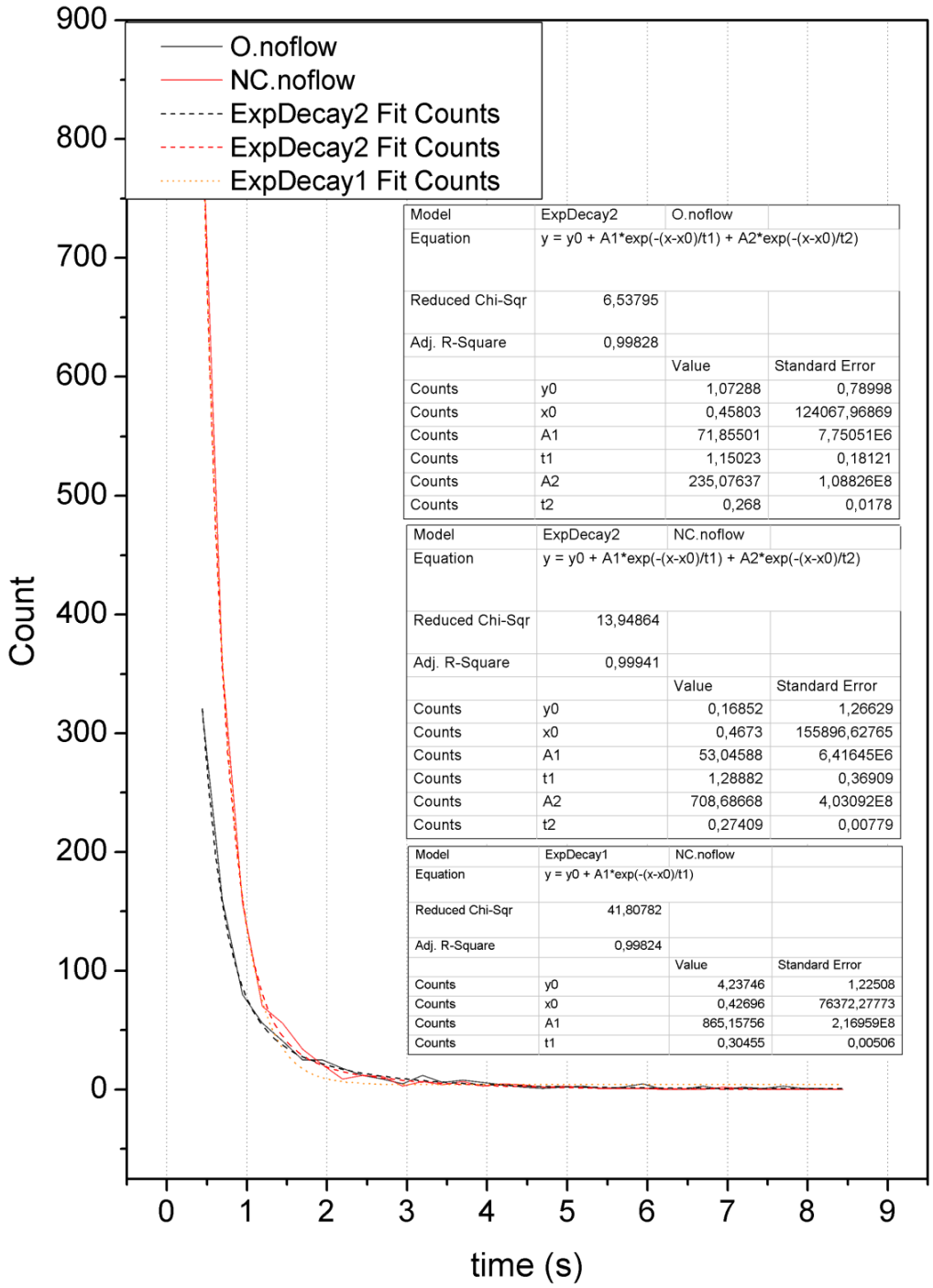

Model	ExpDecay2	O.noflow	
Equation	y = y0 + A1*exp(-(x-x0)/t1) + A2*exp(-(x-x0)/t2)		
Reduced Chi-Sqr	6,53795		
Adj. R-Square	0,99828		
		Value	Standard Error
Counts	y0	1,07288	0,78998
Counts	x0	0,45803	124067,96869
Counts	A1	71,85501	7,75051E6
Counts	t1	1,15023	0,18121
Counts	A2	235,07637	1,08826E8
Counts	t2	0,268	0,0178

Model	ExpDecay2	NC.noflow	
Equation	y = y0 + A1*exp(-(x-x0)/t1) + A2*exp(-(x-x0)/t2)		
Reduced Chi-Sqr	13,94864		
Adj. R-Square	0,99941		
		Value	Standard Error
Counts	y0	0,16852	1,26629
Counts	x0	0,4673	155896,62765
Counts	A1	53,04588	6,41645E6
Counts	t1	1,28882	0,36909
Counts	A2	708,68668	4,03092E8
Counts	t2	0,27409	0,00779

Model	ExpDecay1	NC.noflow	
Equation	y = y0 + A1*exp(-(x-x0)/t1)		
Reduced Chi-Sqr	41,80782		
Adj. R-Square	0,99824		
		Value	Standard Error
Counts	y0	4,23746	1,22508
Counts	x0	0,42696	76372,27773
Counts	A1	865,15756	2,16959E8
Counts	t1	0,30455	0,00506

Figure A.9. **Lifetime distributions for no flow (~0µL/min), Particle Tracker parameters: max. step size = 2, max. slice difference = 2.** Showing lifetime distributions derived from plotting the histograms' count values (from figure A.8) as solid lines. The origami experiment is shown in black colour and negative control in red (and orange) colour. The double exponential and single exponential fits of the distributions are shown as dashed and dotted lines respectively. The fit parameters are shown in the tables in the graph, labelled accordingly.

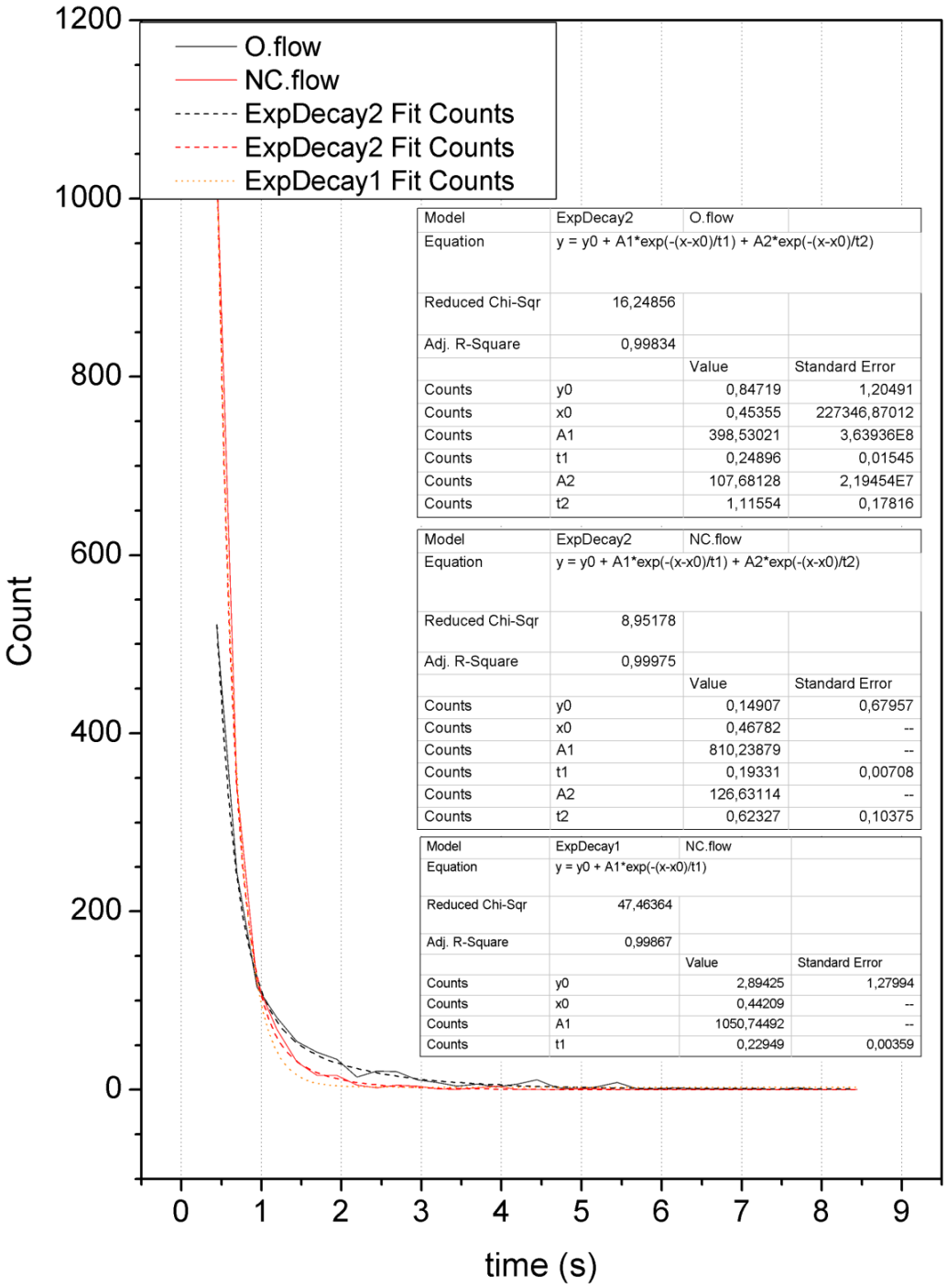

Model	ExpDecay2	O.flow	
Equation	y = y0 + A1*exp(-(x-x0)/t1) + A2*exp(-(x-x0)/t2)		
Reduced Chi-Sqr	16,24856		
Adj. R-Square	0,99834		
		Value	Standard Error
Counts	y0	0,84719	1,20491
Counts	x0	0,45355	227346,87012
Counts	A1	398,53021	3,63936E8
Counts	t1	0,24896	0,01545
Counts	A2	107,68128	2,19454E7
Counts	t2	1,11554	0,17816

Model	ExpDecay2	NC.flow	
Equation	y = y0 + A1*exp(-(x-x0)/t1) + A2*exp(-(x-x0)/t2)		
Reduced Chi-Sqr	8,95178		
Adj. R-Square	0,99975		
		Value	Standard Error
Counts	y0	0,14907	0,67957
Counts	x0	0,46782	--
Counts	A1	810,23879	--
Counts	t1	0,19331	0,00708
Counts	A2	126,63114	--
Counts	t2	0,62327	0,10375

Model	ExpDecay1	NC.flow	
Equation	y = y0 + A1*exp(-(x-x0)/t1)		
Reduced Chi-Sqr	47,46364		
Adj. R-Square	0,99867		
		Value	Standard Error
Counts	y0	2,89425	1,27994
Counts	x0	0,44209	--
Counts	A1	1050,74492	--
Counts	t1	0,22949	0,00359

Figure A.10. **Lifetime distributions with flow (5µL/min), Particle Tracker parameters: max. step size = 2, max. slice difference = 2.** Showing lifetime distributions derived from plotting the histograms' count values (from figure A.8) as solid lines. The origami experiment is shown in black colour and negative control in red (and orange) colour. The double exponential and single exponential fits of the distributions are shown as dashed and dotted lines respectively. The fit parameters are shown in the tables in the graph, labelled accordingly.

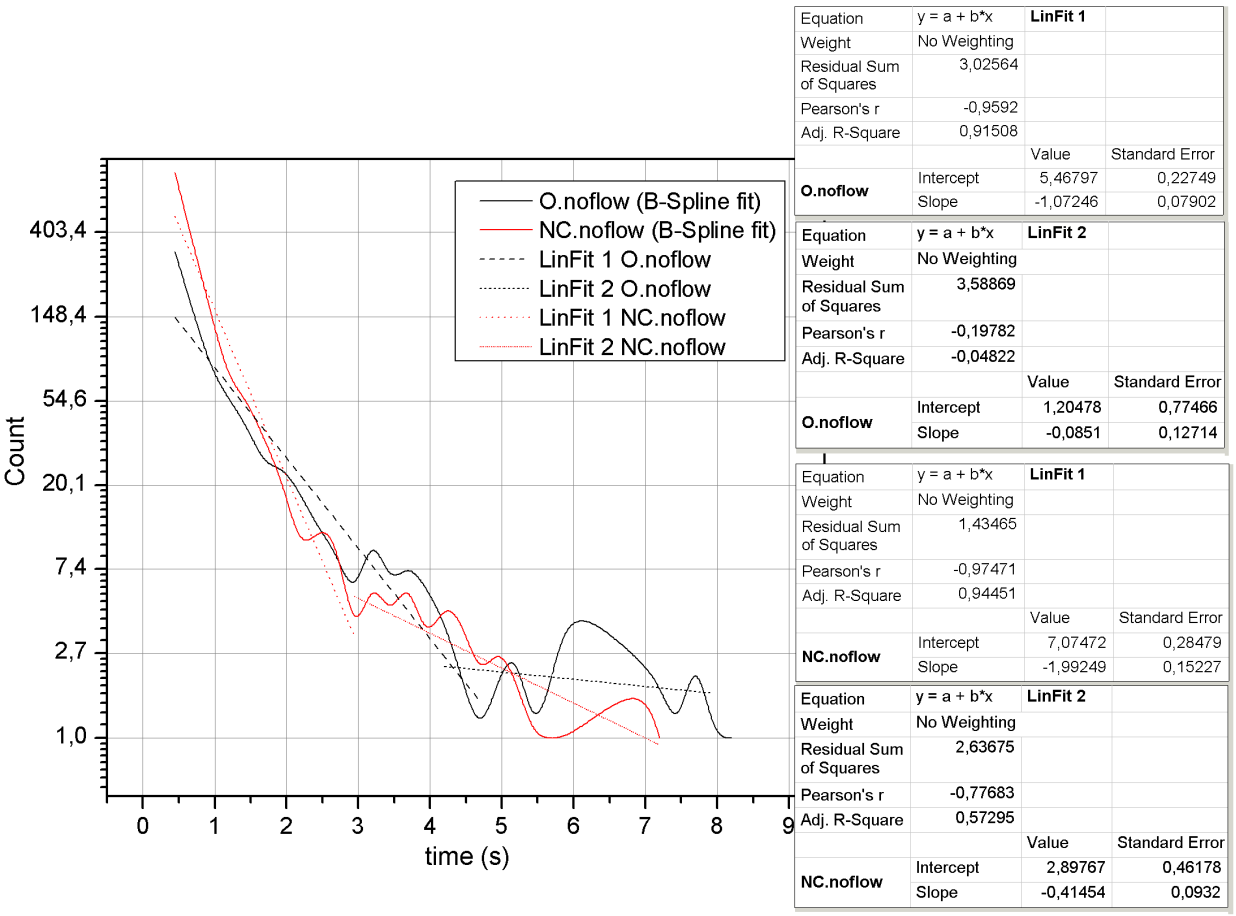

		LinFit 1	
Equation	y = a + b*x		
Weight	No Weighting		
Residual Sum of Squares	3,02564		
Pearson's r	-0,9592		
Adj. R-Square	0,91508		
		Value	Standard Error
O.noflow	Intercept	5,46797	0,22749
	Slope	-1,07246	0,07902

		LinFit 2	
Equation	y = a + b*x		
Weight	No Weighting		
Residual Sum of Squares	3,58869		
Pearson's r	-0,19782		
Adj. R-Square	-0,04822		
		Value	Standard Error
O.noflow	Intercept	1,20478	0,77466
	Slope	-0,0851	0,12714

		LinFit 1	
Equation	y = a + b*x		
Weight	No Weighting		
Residual Sum of Squares	1,43465		
Pearson's r	-0,97471		
Adj. R-Square	0,94451		
		Value	Standard Error
NC.noflow	Intercept	7,07472	0,28479
	Slope	-1,99249	0,15227

		LinFit 2	
Equation	y = a + b*x		
Weight	No Weighting		
Residual Sum of Squares	2,63675		
Pearson's r	-0,77683		
Adj. R-Square	0,57295		
		Value	Standard Error
NC.noflow	Intercept	2,89767	0,46178
	Slope	-0,41454	0,0932

Figure A.11. **Lifetime distributions plotted with single-logarithmic scale (~0μL/min), Particle Tracker parameters: max. step size = 2, max. slice difference = 2.** The origami experimental data is shown in black and negative control in red. The points are connected with a B-Spline fit, for better clarity. Also our attempt of linear fitting to the distributions is shown. This is done in order to estimate the gradients that are present (see fit parameters in tables), but this is much too subjective to conclude anything out of.

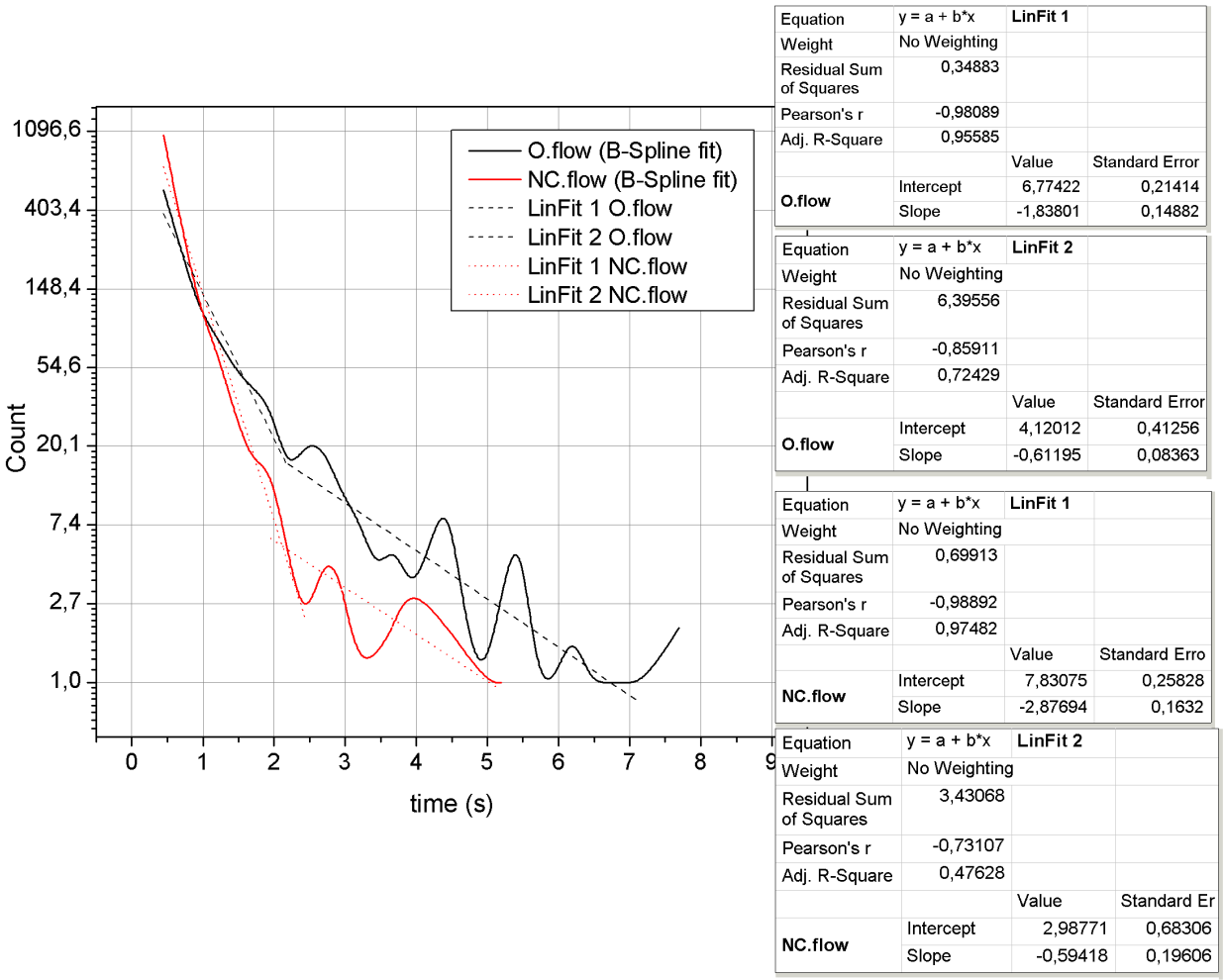

Equation	y = a + b*x	LinFit 1	
Weight	No Weighting		
Residual Sum of Squares	0,34883		
Pearson's r	-0,98089		
Adj. R-Square	0,95585		
		Value	Standard Error
O.flow	Intercept	6,77422	0,21414
	Slope	-1,83801	0,14882

Equation	y = a + b*x	LinFit 2	
Weight	No Weighting		
Residual Sum of Squares	6,39556		
Pearson's r	-0,85911		
Adj. R-Square	0,72429		
		Value	Standard Error
O.flow	Intercept	4,12012	0,41256
	Slope	-0,61195	0,08363

Equation	y = a + b*x	LinFit 1	
Weight	No Weighting		
Residual Sum of Squares	0,69913		
Pearson's r	-0,98892		
Adj. R-Square	0,97482		
		Value	Standard Erro
NC.flow	Intercept	7,83075	0,25828
	Slope	-2,87694	0,1632

Equation	y = a + b*x	LinFit 2	
Weight	No Weighting		
Residual Sum of Squares	3,43068		
Pearson's r	-0,73107		
Adj. R-Square	0,47628		
		Value	Standard Er
NC.flow	Intercept	2,98771	0,68306
	Slope	-0,59418	0,19606

Figure A.12. **Lifetime distributions plotted with single-logarithmic scale (5µL/min), Particle Tracker parameters: max. step size = 2, max. slice difference = 2**. The origami experimental data is shown in black and negative control in red. The points are connected with a B-Spline fit, for better clarity. Also our attempt of linear fitting to the distributions is shown. This is done in order to estimate the gradients that are present (see fit parameters in tables), but this is much too subjective to conclude anything out of.

- Particle Tracker parameters: max. step size = 2, max. slice difference = 1.

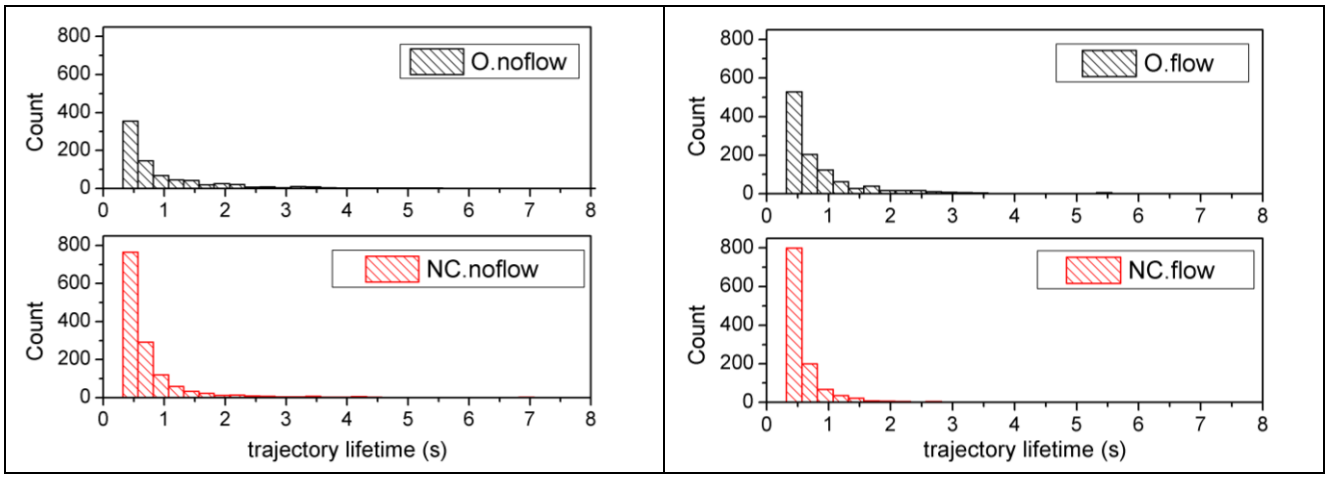

Figure A.13. **Histograms of the trajectory lifetimes, Particle Tracker parameters: max. step size = 2, max. slice difference = 1.** Data is collected from two or three separate movies for every histogram shown. On the left hand side is the origami (black) and negative control (red) data for no active flow (~0µL/min). On the right hand side the data with active flow (5µL/min).

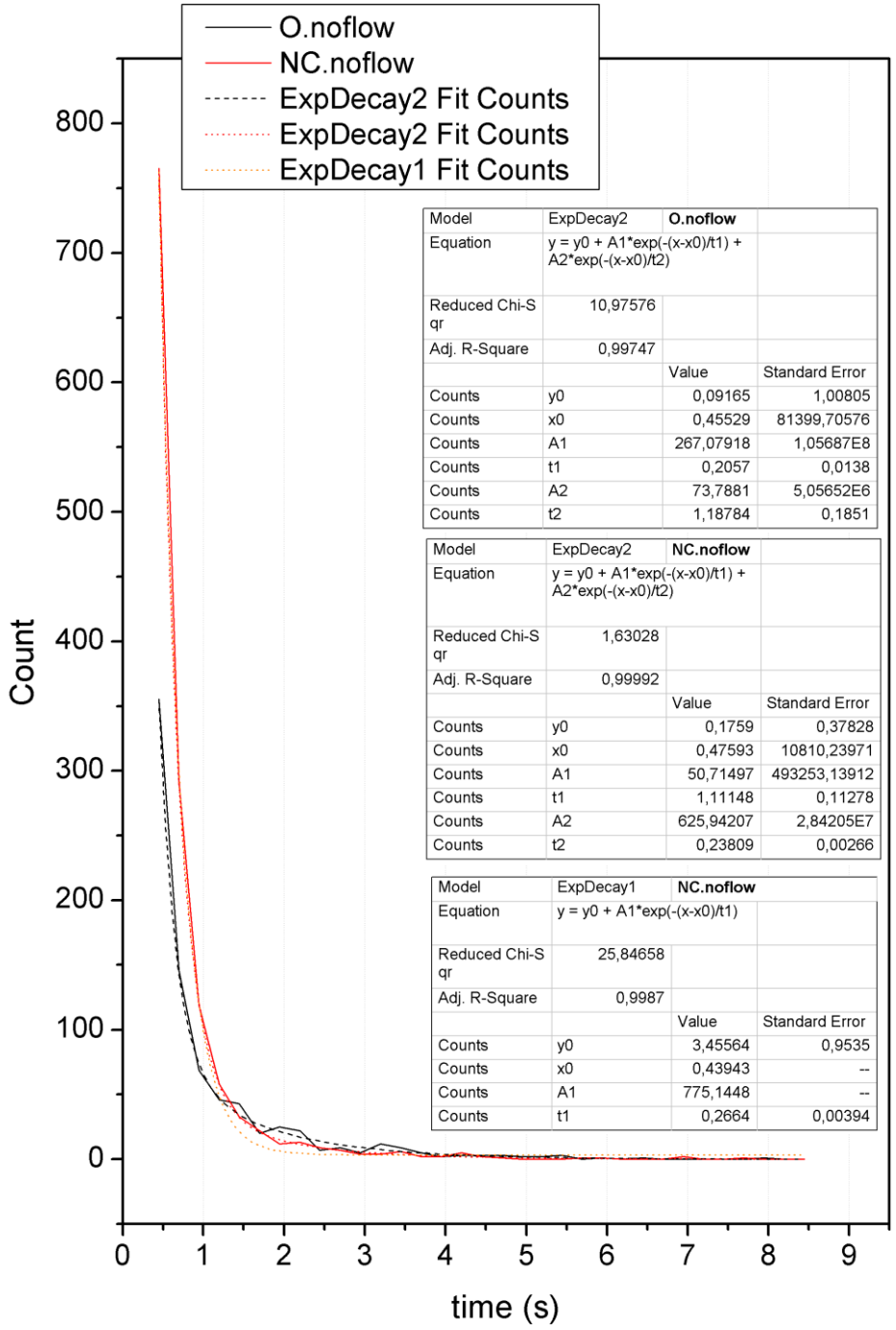

Model	ExpDecay2	O.noflow	
Equation	y = y0 + A1*exp(-(x-x0)/t1) + A2*exp(-(x-x0)/t2)		
Reduced Chi-Sqr	10,97576		
Adj. R-Square	0,99747		
		Value	Standard Error
Counts	y0	0,09165	1,00805
Counts	x0	0,45529	81399,70576
Counts	A1	267,07918	1,05687E8
Counts	t1	0,2057	0,0138
Counts	A2	73,7881	5,05652E6
Counts	t2	1,18784	0,1851

Model	ExpDecay2	NC.noflow	
Equation	y = y0 + A1*exp(-(x-x0)/t1) + A2*exp(-(x-x0)/t2)		
Reduced Chi-Sqr	1,63028		
Adj. R-Square	0,99992		
		Value	Standard Error
Counts	y0	0,1759	0,37828
Counts	x0	0,47593	10810,23971
Counts	A1	50,71497	493253,13912
Counts	t1	1,11148	0,11278
Counts	A2	625,94207	2,84205E7
Counts	t2	0,23809	0,00266

Model	ExpDecay1	NC.noflow	
Equation	y = y0 + A1*exp(-(x-x0)/t1)		
Reduced Chi-Sqr	25,84658		
Adj. R-Square	0,9987		
		Value	Standard Error
Counts	y0	3,45564	0,9535
Counts	x0	0,43943	--
Counts	A1	775,1448	--
Counts	t1	0,2664	0,00394

Figure A.14. **Lifetime distributions for no flow (~0µL/min), Particle Tracker parameters: max. step size = 2, max. slice difference = 1**. Showing lifetime distributions derived from plotting the histograms' count values (from figure A.13) as solid lines. The origami experiment is shown in black colour and negative control in red (and orange) colour. The double exponential and single exponential fits of the distributions are shown as dashed and dotted lines respectively. The fit parameters are shown in the tables in the graph, labelled accordingly.

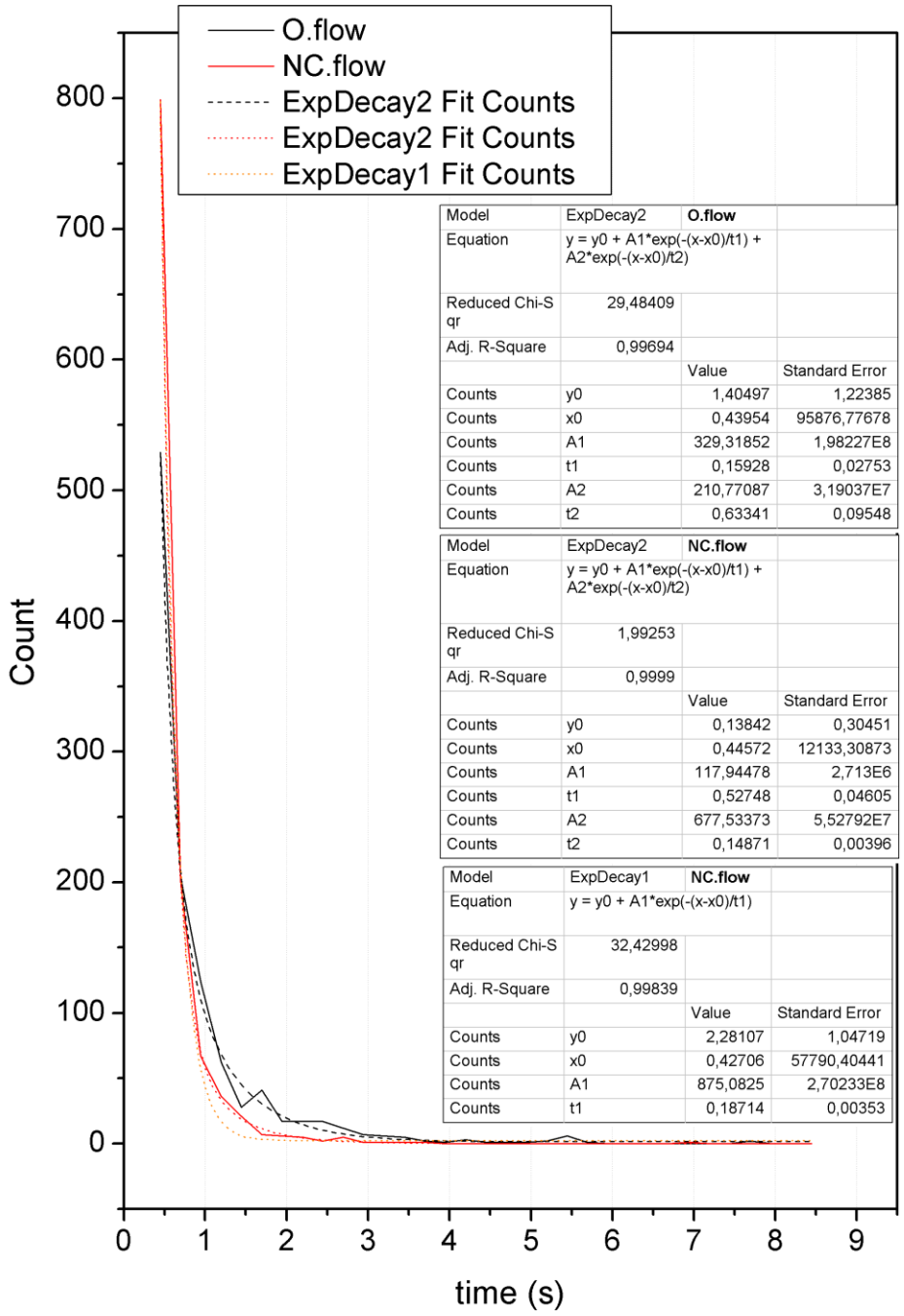

Figure A.15. **Lifetime distributions with flow (5μL/min), Particle Tracker parameters: max. step size = 2, max. slice difference = 1**. Showing lifetime distributions derived from plotting the histograms' count values (from figure A.13) as solid lines. The origami experiment is shown in black colour and negative control in red (and orange) colour. The double exponential and single exponential fits of the distributions are shown as dashed and dotted lines respectively. The fit parameters are shown in the tables in the graph, labelled accordingly.

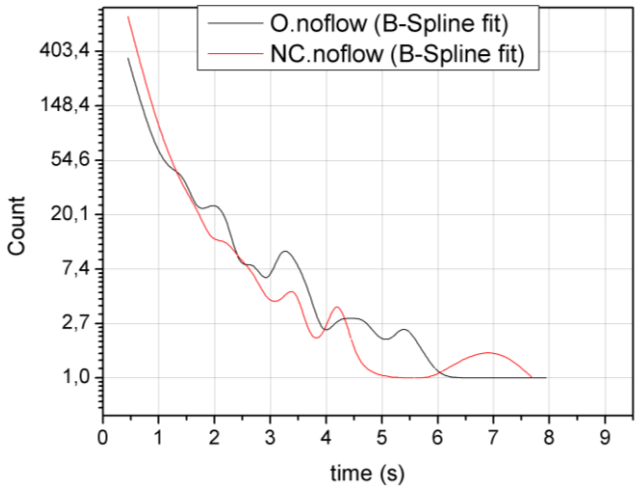

Figure A.16. **Lifetime distributions plotted with single-logarithmic scale (~0μL/min), Particle Tracker parameters: max. step size = 2, max. slice difference = 1**. The origami experimental data is shown in black and negative control in red. The points are connected with a B-Spline fit, for better clarity.

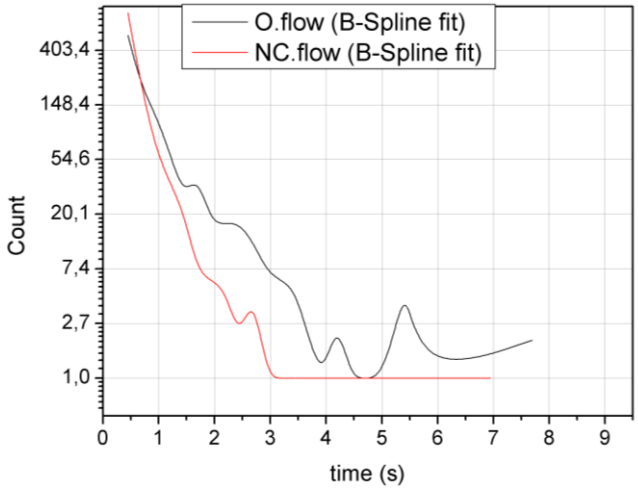

Figure A.17. **Lifetime distributions plotted with single-logarithmic scale (5μL/min), Particle Tracker parameters: max. step size = 2, max. slice difference = 1**. The origami experimental data is shown in black and negative control in red. The points are connected with a B-Spline fit, for better clarity.

- Particle Tracker parameters: max. step size = 1, max. slice difference = 2.

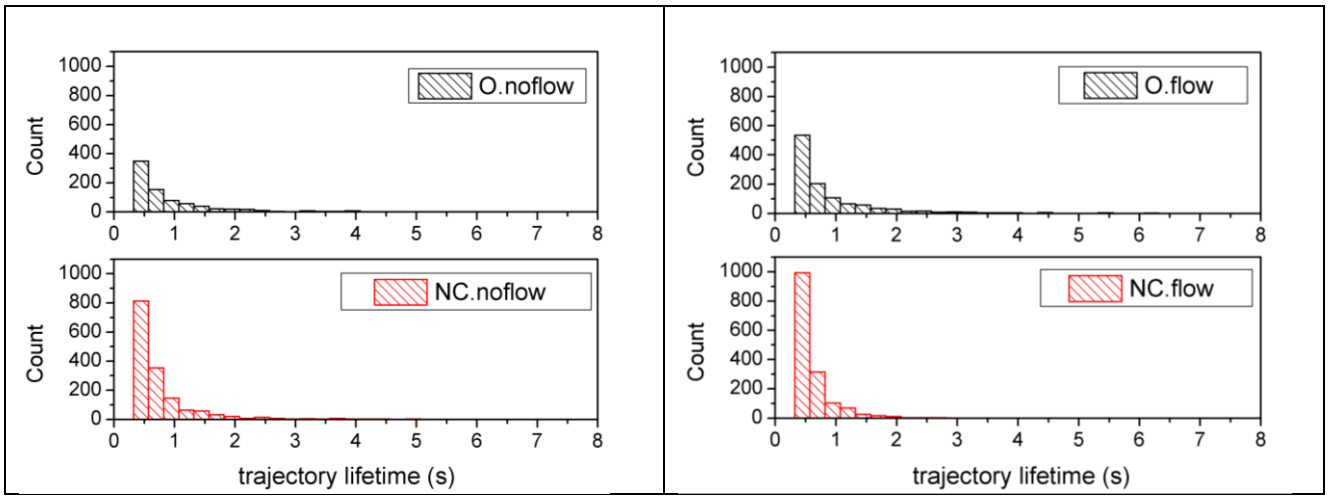

Figure A.18. **Histograms of the trajectory lifetimes, Particle Tracker parameters: max. step size = 1, max. slice difference = 2.** Data is collected from two or three separate movies for every histogram shown. On the left hand side is the origami (black) and negative control (red) data for no active flow (~0μL/min). On the right hand side the data with active flow (5μL/min).

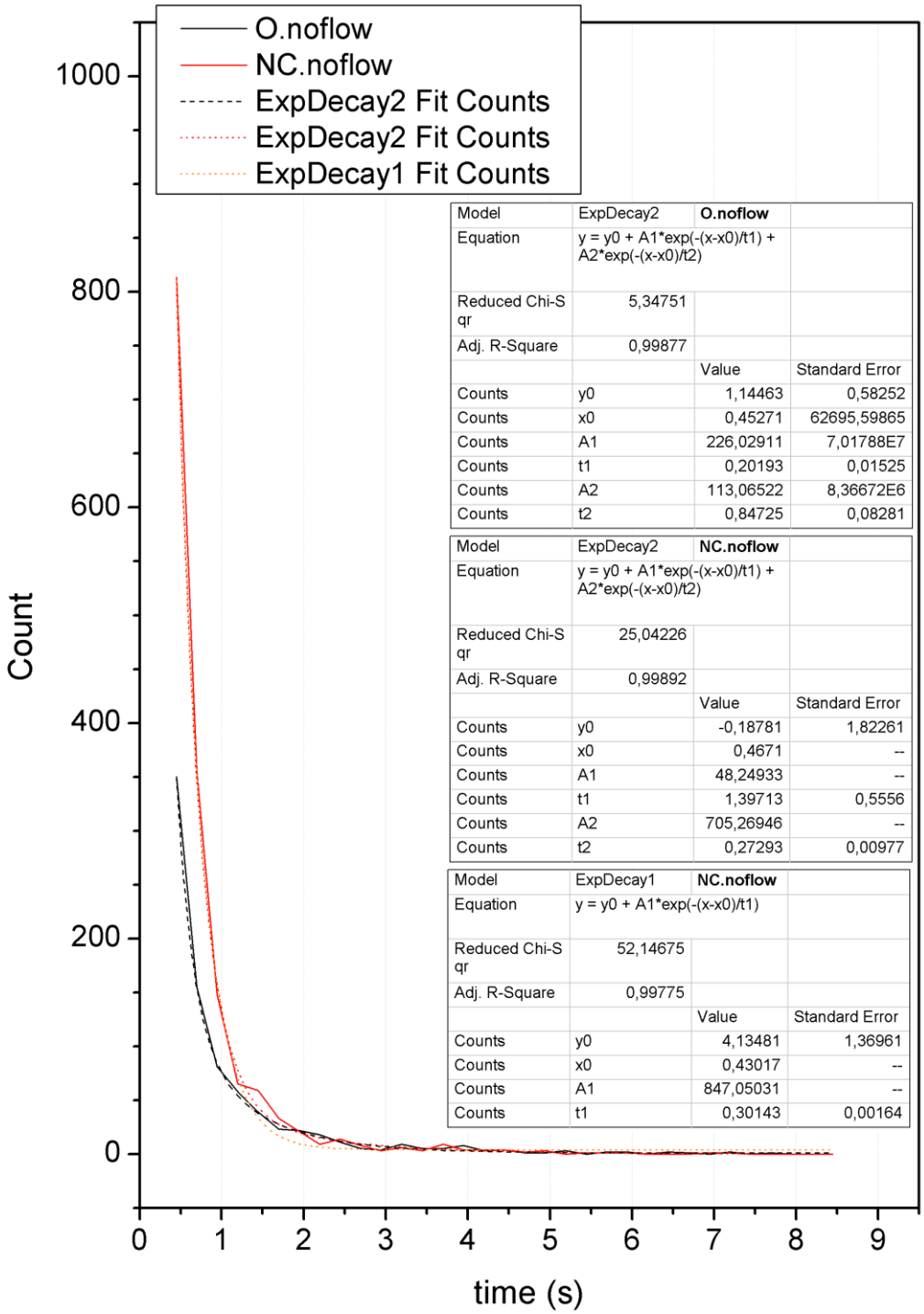

Model	ExpDecay2	**O.noflow**	
Equation	y = y0 + A1*exp(-(x-x0)/t1) + A2*exp(-(x-x0)/t2)		
Reduced Chi-Sqr	5,34751		
Adj. R-Square	0,99877		
		Value	Standard Error
Counts	y0	1,14463	0,58252
Counts	x0	0,45271	62695,59865
Counts	A1	226,02911	7,01788E7
Counts	t1	0,20193	0,01525
Counts	A2	113,06522	8,36672E6
Counts	t2	0,84725	0,08281

Model	ExpDecay2	**NC.noflow**	
Equation	y = y0 + A1*exp(-(x-x0)/t1) + A2*exp(-(x-x0)/t2)		
Reduced Chi-Sqr	25,04226		
Adj. R-Square	0,99892		
		Value	Standard Error
Counts	y0	-0,18781	1,82261
Counts	x0	0,4671	--
Counts	A1	48,24933	--
Counts	t1	1,39713	0,5556
Counts	A2	705,26946	--
Counts	t2	0,27293	0,00977

Model	ExpDecay1	**NC.noflow**	
Equation	y = y0 + A1*exp(-(x-x0)/t1)		
Reduced Chi-Sqr	52,14675		
Adj. R-Square	0,99775		
		Value	Standard Error
Counts	y0	4,13481	1,36961
Counts	x0	0,43017	--
Counts	A1	847,05031	--
Counts	t1	0,30143	0,00164

Figure A.19. **Lifetime distributions for no flow (~0μL/min), Particle Tracker parameters: max. step size = 1, max. slice difference = 2**. Showing lifetime distributions derived from plotting the histograms' count values (from figure A.18) as solid lines. The origami experiment is shown in black colour and negative control in red (and orange) colour. The double exponential and single exponential fits of the distributions are shown as dashed and dotted lines respectively. The fit parameters are shown in the tables in the graph, labelled accordingly.

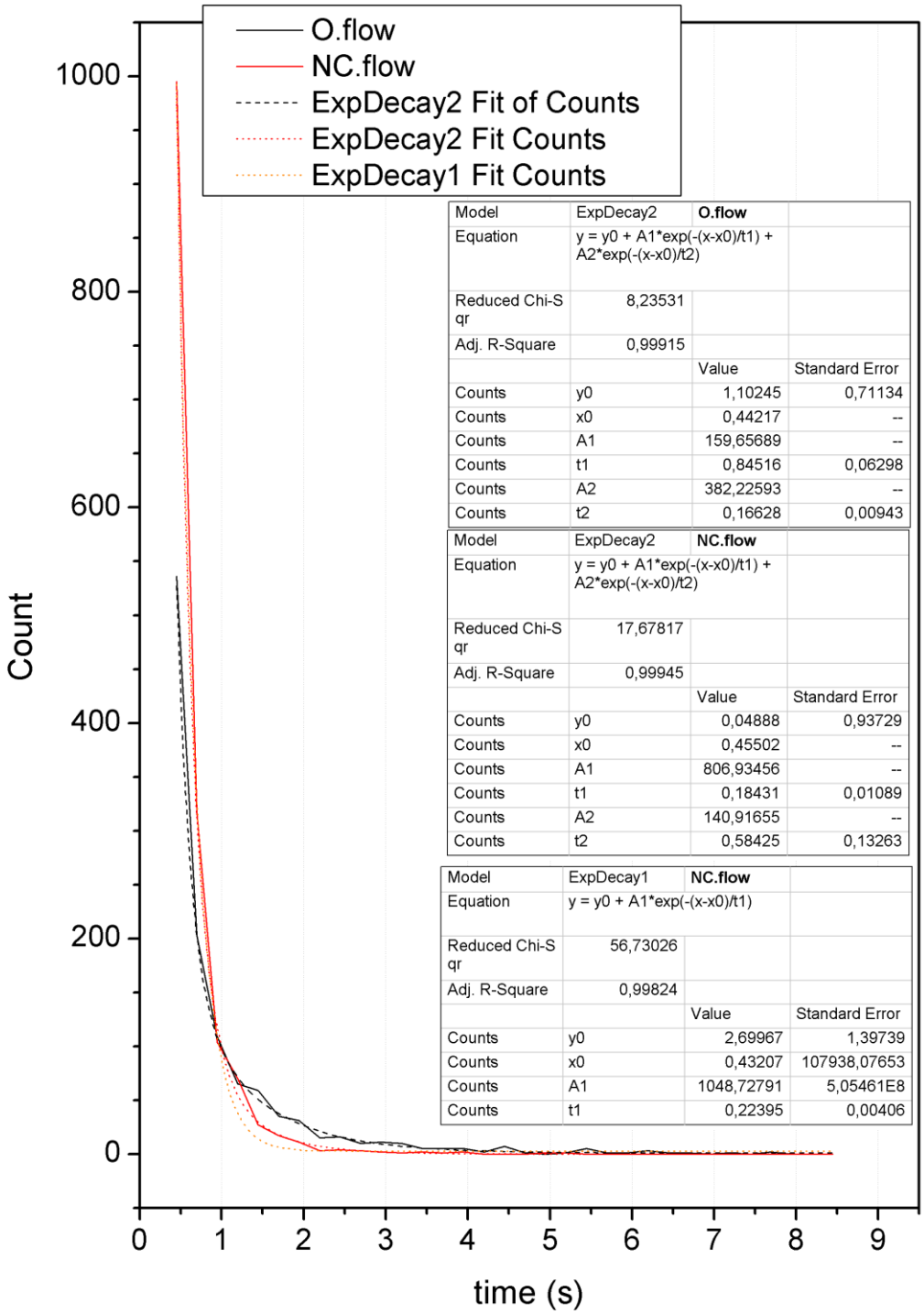

Model	ExpDecay2	**O.flow**	
Equation	y = y0 + A1*exp(-(x-x0)/t1) + A2*exp(-(x-x0)/t2)		
Reduced Chi-Sqr	8,23531		
Adj. R-Square	0,99915		
		Value	Standard Error
Counts	y0	1,10245	0,71134
Counts	x0	0,44217	--
Counts	A1	159,65689	--
Counts	t1	0,84516	0,06298
Counts	A2	382,22593	--
Counts	t2	0,16628	0,00943

Model	ExpDecay2	**NC.flow**	
Equation	y = y0 + A1*exp(-(x-x0)/t1) + A2*exp(-(x-x0)/t2)		
Reduced Chi-Sqr	17,67817		
Adj. R-Square	0,99945		
		Value	Standard Error
Counts	y0	0,04888	0,93729
Counts	x0	0,45502	--
Counts	A1	806,93456	--
Counts	t1	0,18431	0,01089
Counts	A2	140,91655	--
Counts	t2	0,58425	0,13263

Model	ExpDecay1	**NC.flow**	
Equation	y = y0 + A1*exp(-(x-x0)/t1)		
Reduced Chi-Sqr	56,73026		
Adj. R-Square	0,99824		
		Value	Standard Error
Counts	y0	2,69967	1,39739
Counts	x0	0,43207	107938,07653
Counts	A1	1048,72791	5,05461E8
Counts	t1	0,22395	0,00406

Figure A.20. **Lifetime distributions with flow (5µL/min), Particle Tracker parameters: max. step size = 1, max. slice difference = 2**. Showing lifetime distributions derived from plotting the histograms' count values (from figure A.18) as solid lines. The origami experiment is shown in black colour and negative control in red (and orange) colour. The double exponential and single exponential fits of the distributions are shown as dashed and dotted lines respectively. The fit parameters are shown in the tables in the graph, labelled accordingly.

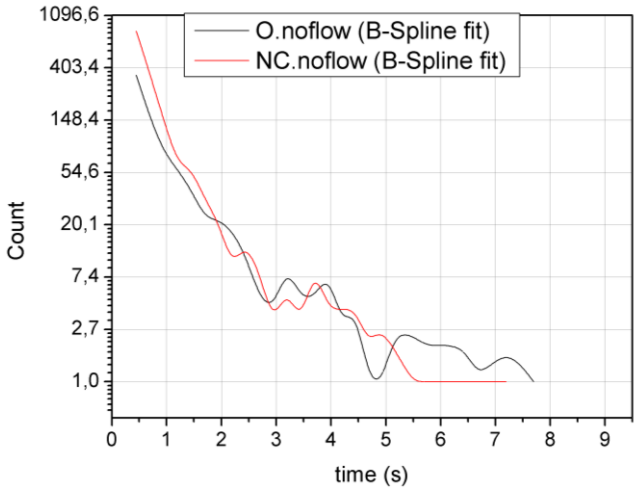

Figure A.21. **Lifetime distributions plotted with single-logarithmic scale (~0μL/min), Particle Tracker parameters: max. step size = 1, max. slice difference = 2**. The origami experimental data is shown in black and negative control in red. The points are connected with a B-Spline fit, for better clarity.

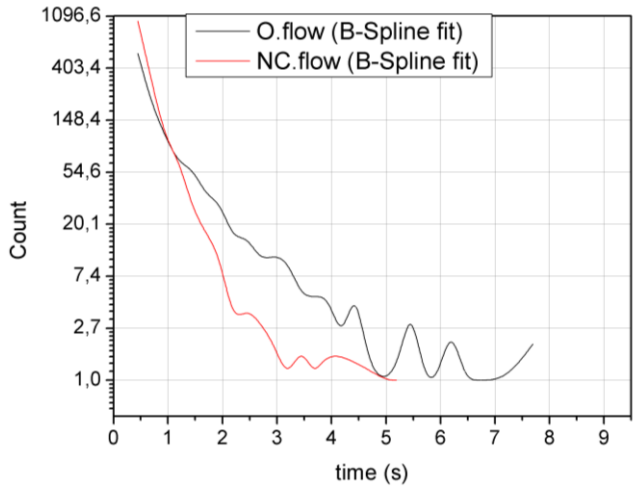

Figure A.22. **Lifetime distributions plotted with single-logarithmic scale (5μL/min), Particle Tracker parameters: max. step size = 1, max. slice difference = 2.** The origami experimental data is shown in black and negative control in red. The points are connected with a B-Spline fit, for better clarity.

Appendix B: Field of View (FOV) oscillations

While pursuing a lower exposure time we stumbled upon the phenomenon that all the spots in the 32x256 pixel FOV were oscillating together uniformly in a sinusoidal fashion. The displacement of the oscillation was only observable in the y-direction, perpendicular to the flow through the channel. From the kymograph of one particle we calculated the approximate period (averaging over different sections and several periods) which gave a frequency of approximately 70Hz (+- 5Hz). The amplitude is estimated at roughly 80nm.

This immediately gives an explanation to the wider FWHM of the y-direction Gaussian fit of the fluorescent spots (larger mean value of the histogram). This is because when using a 16,01ms exposure time the sampling rate is not fast enough and oscillations are summed up into one single spot.

Strangely enough this has so far been observed to affect only the origami experiment and not the negative control or Streptavidin-Cy5 control experiments. Further negative control and streptavidin-Cy5 control experiments at low exposure time are necessary to make complete judgement.

Furthermore we have tried to localize where these oscillations come from. The following facts have been observed from further investigations and experiments:

- The bright field experiment is not affected by this oscillatory motion, only the camera and LED microscope light was on.

- Only 4.21ms exposure time was used to quantify the oscillations.

- The flow does not cause these oscillations. Even when the syringe pump settings were altered and the flow tubing was disconnected the oscillations were present.

- All the equipment (with exception of the laser and camera) were switched off, they do not affect the oscillation.

- It was not controlled whether exposure times and FOV size (actually only software settings which should not make a difference) are affecting the oscillations.

Guidelines and suggestions for further analysis of this problem:

- Check whether this artefact arises from the camera itself (maybe due to the cooling fans mechanical oscillations? Try out water cooling, which also reduces thermal noise).

- Control another microscope setup, does it also show such oscillations.

- Different experiments

- Is it possible that is an optical effect that we observe?